Environment International 174 (2023) 107885

Contents lists available at ScienceDirect

Environment International

journal homepage: www.elsevier.com/locate/envint

Review article

Sampling strategies and analytical techniques for assessment of airborne micro and nano plastics

Aala Azari [a], Jeroen A.J. Vanoirbeek [a], Frank Van Belleghem [b], Brent Vleeschouwers [a], Peter H.M. Hoet [a,*], Manosij Ghosh [a,*,1]

[a] Environment and Health, Department of Public Health and Primary Care, KU Leuven, Herestraat 49, 3000 Leuven, Belgium
[b] Centre for Environmental Sciences, Department of Biology, Hasselt University Hasselt, Belgium

ARTICLE INFO

Handling Editor: Xavier Querol

Keywords:
Microplastics
Nano plastics
Atmosphere
Analytical methods

ABSTRACT

The atmosphere is pervasively polluted by microplastics and nano plastics (M/NPs) released into indoor and outdoor areas. However, various methodologies and their limitations along with non-standardization make the comparison of information concerning their prevalence difficult. Such diversity in techniques greatly limits the interpretation of results. Herein, We extracted data from publications on PubMed and Embase database up to the year 2022 regarding sampling strategies, identification methods, and reporting data for M/NPs quantification. In this review, 5 major areas for measuring airborne M/NPs have been identified including pre-sampling/ sampling/ post-sampling/ analysis/ and contamination avoidance. There are many challenges specific to each of those sections that need to be resolved through further method development and harmonization. This review mainly focuses on the different methods for collecting atmospheric M/NPs and also the analytical tools which have been used for their identification. While passive sampling is the most user-friendly method, the most precise and reproducible approach for collecting plastic particles is an active method which is directly followed by visual counting as the most common physical analysis technique. Polymers collected using visual sorting are most frequently identified by spectroscopy (FTIR; Raman). However, destructive analytical techniques (thermal degradation) also provide precise chemical information. In all cases, the methods were screened for advantages, limitations, and fieldwork abilities. This review outlines and critiques knowledge gaps, and recommendations to support standardized and comparable future research.

1. Introduction

Based on the ISO (International Organization for Standardization) definition, plastics are high polymer substances that can be shaped by flow from the processing stage to the final product. However, the popular synonym for plastics: synthetic macromolecular materials, includes plastic and rubber. As plastics are produced and used in large quantities globally in different sectors such as packaging, construction and, transport, it is expected that 12 billion tons of plastic waste will be generated by 2050. As a result, the environment is becoming increasingly polluted with plastics and plastic waste, partly as a result of improper waste management (Dümichen et al. 2017).

As plastic polymers are highly resistant to aging they persist in the environment for multiple decades where they are exposed to factors like sunlight, oxidizing atmosphere, and mechanical stress, leading to degradation into tiny particles and fibers called microplastics (MPs)

Abbreviations: a.s.L., above the sea level; CaF2, calcium fluoride; C/O, Carbon to oxygen ratio; FTIR, Fourier-transform infrared spectroscopy; HQI, Hit Quality Index; LOD, Limit of detection; MRs, micro rubbers; MP, Microplastics Micro and nano plastics; μFT-IR, Micro- Fourier-transform infrared spectroscopy; NP, Nano plastics M/NPs; PLM, polarized light microscopy; PA, Polyamide; PEST, Polyesters; PE, Polyethylene; PET, Polyethylene terephthalate; PP, Polypropylene; PS, Polystyrene (); PTEF, Polytetrafluoroethylene; PVC, poly(vinyl chloride); Pyr-GC/MS, Pyrolysis gas chromatography-mass spectrometry; RH, relative humidity; S&S, Schleicher & Schuell; SEM, scanning electron microscope; SEM-EDX, Scanning Electron Microscopy- Energy Dispersive X-Ray Analysis; TED-GC/MS, Thermal extraction and desorption gas chromatography-mass spectrometry; TGA-GC/MS, thermogravimetric analysis gas chromatography-mass spectrometry; v/v, volume per volume; w/w, weight per weight; ZnSe, Zinc Selenide.

* Corresponding authors.
E-mail addresses: peter.hoet@kuleuven.be (P.H.M. Hoet), manosij.ghosh@kuleuven.be (M. Ghosh).
[1] Environment and Health, Department of Public Health and Primary Care, KU Leuven, Herestraat 49, 3000 Leuven, Belgium.

https://doi.org/10.1016/j.envint.2023.107885
Received 7 November 2022; Received in revised form 13 March 2023; Accepted 15 March 2023
Available online 23 March 2023

(Ding et al., 2021a; Dümichen et al. 2017; Wright et al. 2019). Based on the ISO definition, MPs refer to water-insoluble solid plastic particles with any dimension between 1 mm and 5 mm (Plastics 2020). More recently, a distinction has been made between MPs (5 mm- 1 μm) and nano plastics (NPs) < 1 μm (Abbasi & Turner 2021a; Gigault et al. 2018; González-Pleiter et al., 2021; I. S. O. 2020).

MPs and NPs (M/NPs) can be categorized as primary or secondary plastics. Primary M/NPs are polymers intentionally manufactured in small sizes, e.g. cosmetics, medicinal ingredients and raw materials used for plastic production(Mattsson et al. 2018; Turner & Holmes 2011). Secondary ones are products of the degradation of larger plastic fragments including fibers from synthetic textiles (Mattsson et al. 2018; Szewc et al. 2021a). M/NPs can exist in a number of different shapes, including pellets, films, foams, fragments, granules, and fibers, whose shapes and forms are largely dependent on their source. Moreover, they vary in length, diameter, color, and polymer type (Welsh et al. 2022).

A variety of studies indicate different numbers and concentrations of M/NPs in all types of media, from soils to aquatic systems, in the general environment to the digestive tracts of vertebrates and invertebrates (Eriksen et al. 2013; Free et al. 2014; Mani et al. 2016; Mattsson et al. 2018; Scheurer & Bigalke 2018; Zhang & Liu 2018). In freshwater, seawater, soil, and sediment, MPs are found at levels of 10–5–10 items/L, 10–6–10 items/L, 1–104 items/Kg, and 1–103 items/Kg, respectively (Liu et al. 2022a). It was illustrated that the coastal beach soil in China contains 1.3 to 14712.5 MPs/Kg (He et al. 2018). Moreover, the concentration of MPs found in the harbors was up to 390 MPs/Kg of dry sediment along the Belgian coast (Claessens et al. 2011). Bottled drinking water contains MPs ranging from 14 to 4889 MPs/L based on the type of the container and there are much fewer MPs in tape water ranging from 2 to 930 MPs/L (Oßmann 2021). Microplastic particles have also been reported in marine products like shrimp, fish, oysters, and salt(Qu et al. 2023). As a consequence, several pathways can lead to human exposure to microplastics, including ingestion of food and water (Qu et al. 2023).

Due to the small size and low density (0.9–1.4 g cm^{-3} for most common plastics), MPs can also be suspended in the atmosphere by wind or air turbulence and remain in the atmosphere for long periods of time (Ferrero et al. 2022). Therefore, airborne MPs can also pose a potential health threat to humans as inhaled particles may lead to chronic inflammation and non-malignant and malignant lung disease (Szewc et al. 2021a). While the majority of research focuses on outdoor M/NPs (Huang et al., 2021; Kernchen et al. 2022; Wang et al. 2020; Welsh et al. 2022), some studies identify indoor dust as a non-negligible source of human exposure to MPs (O'Brien et al. 2020; Soltani et al., 2021a, 2021b; Vianello et al. 2019).

One of the major concerns hindering our understanding of the plastic cycle is the issue of sampling, measuring and, investigating M/NPs in the atmosphere. Comparison of the multitude of studies on M/NPs is currently limited due to a lack of harmonization of the methods used for sampling, identification and, characterization. To have a better comprehension of the current state of atmospheric M/NPs, it is essential to collect and compare current research findings. This in turn can lead to a better understanding of the current state of knowledge and compare atmospheric M/NPs characteristics with M/NPs from other environments. The current review on atmospheric M/NPs is therefore focusing on sampling, sample preparation and identification methods. The approach will enable knowledge gaps to be identified, and recommendations to be made to support standardized and comparable future research.

2. Methodology

2.1. Search strategy

An electronic systematic search of PubMed and EMBASE was performed to identify articles examining the analytical methods for M/NPs identification and characterization. We searched for relevant publications in English, in two separate periods. Databases were searched for published papers for a period of 10 years (August 4, 2011, to August 4, 2021). As the field is rapidly evolving, a second search was conducted from August 1, 2021 to April 30, 2022. A manual search for references cited by the identified studies was also undertaken. Medical subject headings (MeSH) and keywords included: "MPs" OR "MP*" OR "nanoplastic*" OR "nano plastic*" OR "MP" OR "MPs" OR "NP"OR "NPs" OR "MP NP" OR "MPs NPs" OR "synthetic fibre*" OR "synthetic fiber*" OR "plastic fibre*" OR "plastic fibre*" OR "synthetic textile*" OR "plastic particle*" OR "plastic debris" AND ("Atmosphere" OR "Air" OR "airborne" OR "indoor air" OR "outdoor air" OR "atmospher*" OR "atmospheric fallout" OR "atmospheric deposition" AND ("sampl*" OR "deposition sampl*" OR "treatment" OR "pretreatment"[Title/Abstract] OR "measur*" AND "analys*" OR "microscopy"OR "spectroscopy" OR "microspectroscopy" OR "spectrometry" OR "chromatography" OR "scattering" OR "electrophoresis" OR "raman" (see Appendix for complete search strategy).

2.2. Eligibility criteria

To be included in the review, a published study had to meet the following criteria: original article, atmospheric micro- and nano plastics, sampling, analytical method, and identification and characterization. To determine the eligibility of the identified studies, the abstracts of the 41 identified studies were screened and the full text of the article was reviewed when the abstract did not provide sufficient information.

2.3. Exclusion criteria

Published studies that met the following criteria were excluded from our search: (1) review articles; (2) M/NPs from "media" other than air or atmosphere; (3) human studies; (4) in vitro studies; (5) animal studies.

As the field of research is rapidly emerging, a first search was conducted in 2021, followed by a second search in 2022. The PRISMA 2020 flow of study selection is shown in Fig. 1(Page et al. 2021). A total of 639 and 228 articles were retrieved from PubMed and Embase, respectively. In the second step, 112 and 46 duplicates were removed from the first and second periods of our search, respectively. In a third step, we screened the title and abstract by using exclusion criteria to select studies that matched our search line. After title/abstract screening, 15 and 13 articles were retained for data extraction from each period of our search. In a final step, 13 papers were added to the review through snowballing. Finally, a total of 41 papers were selected for the review.

2.4. Data extraction

All data in the 41 studies were extracted using a custom-built database. Any discrepancies were discussed and resolved. The following study characteristics were recorded: year of publication, country of origin, name of the authors, the title of the study, journal of the publication, aim of the study, location characteristics (type of environment, study location, sampling point, sampling height, sampling period), sampling duration, number of samples, volume of samples, blanks, collection of samples, type of sampler, filters, pretreatment procedure, environmental factors, deposition rate, quality assurance, and contamination avoidance, verification tools, trajectory analysis, quantification and concentration, physical and chemical characteristics, data analysis and statistical analysis and other results.

3. Results

3.1. Important pre-sampling considerations in airborne M/NPs sampling

3.1.1. Matrix and type of environment

According to the search string, all articles focused on airborne M/

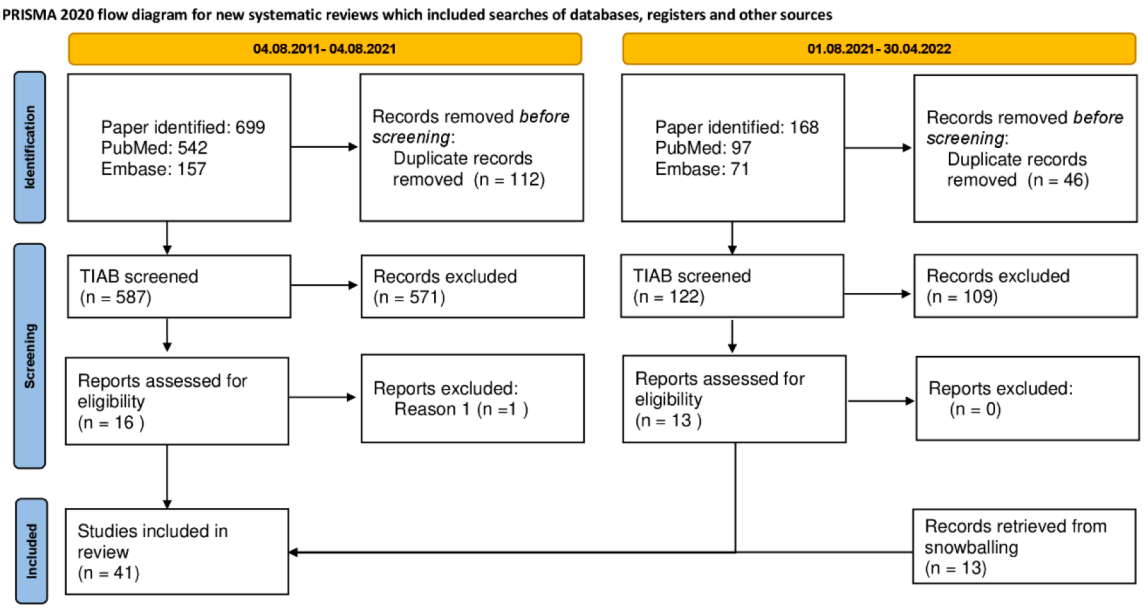

Fig. 1. PRISMA 2020 Flow diagram of the search strategy used for this review. Reason 1: analyzing the MPs in other environments rather than the air.

NPs. The matrix from which particles were collected includes air, water (rain or snow), and dust (Supplementary table 1). While 26 studies collected M/NP directly from the air through different sampling methods, 6 studies collected MP in precipitation, of which 5 were from rain water and 1 from snow. Moreover, in 4 articles M/NPs were collected from both the air and water matrix Along with this, 4 papers focused on particles in settled dust, one paper on both air and settled dust matrix and one worked on rain water and settled dust.

3.1.2. Study area

Given the aim of the study, airborne MPs can be assessed in either indoor or outdoor environments. Although most papers focused on the outdoor environment, 7 studies analyzed MPs in indoor settings, and 6 studied both indoor and outdoor MPs (Supplementary table 1). Several studies showed that MPs are ubiquitous in both urbanized and non-urbanized environments which can affect human health (González-Pleiter et al., 2021; Kernchen et al. 2022; Liao et al. 2021). Based on the living location of the population, 17 outdoor studies, 2 indoor studies, and 3 mixed-setting studies evaluated MPs in urbanized situations identified as different areas including residential areas, industrial areas, public gardens, commercial areas, main traffic roads, and transportation hubs. In addition to urban settings, 6 studies have been performed in specific remote areas like oceans, lakes, and mountains. The reviewed studies also show that in order to identify MP abundance in an indoor environment, it is essential to identify accurate characteristics of the place under study such as type of the rooms, number of the room in the area, number of occupants and their age, main floor covering, number of windows and doors and their opening or closing situation, and air conditioning, ventilation, and heating system (O'Brien et al. 2020; Soltani et al., 2021a, 2021b; Vianello et al. 2019; Xie et al. 2022, Yao et al., 2022). In addition, in an experiment conducted by (Soltani et al., 2021a, 2021b), the role of cleaning in reducing MPs loads in the home was demonstrated through a significant difference between the frequency of use of vacuum cleaners. In addition, they showed a correlation between traffic density (outside) and indoor deposition rate of MPs.

3.1.3. Type of sampling

Generally, there are two types of sampling methods; passive and active, each suitable for a specific purpose. According to our search, 15 articles utilized active sampling, and 20 articles used passive one (Table 1).

Passive: For passive sampling, which is specifically used for the analysis of deposition of M/NPs, it is important to investigate the number of airborne M/NPs in wet and dry atmospheric deposition in order to estimate the total load of M/NPs input into the environment (Rocha-Santos et al. 2022). Methods and instruments for passive sampling include a bottle with a funnel attached (8 studies), an open beaker or bucket (3 studies), a petri dish (3 studies) covered with adhesive, a pan and brush (5 studies) and an automated wet deposition sampler (one study) (Table 2). The funnel over a bottle and open beaker have been shown to be equally reliable and low-cost methods for collecting atmospheric fallout. The lip of the beaker is just as effective as the funnel in preventing particle resuspension, and it may be easier for particles to enter the beaker compared to the funnel (Knobloch et al. 2021a).

Active: Although the active sampling method requires specialized equipment and infrastructures, like the energy input, it can result in an accurate determination of MP per air volume and is therefore also highly reproducible (Rocha-Santos et al. 2022) if a sufficient volume (more than 70 m^3) is sampled (Liu et al. 2019b). According to our review, there were 6 papers with comprehensive data (Table 3) on sampling flow rate, the volume of air sampled and sampling duration (Kernchen et al. 2022; Liao et al. 2021; Liu et al. 2019a; Vianello et al. 2019; Wang et al. 2020; Xie et al. 2022).

Combination of active and passive sampling: To comprehensively assess atmospheric M/NPs pollution, the simultaneous use of both passive and active sampling methods is recommended (Ding et al., 2021a). Passive and active sampling, in particular, are supplementary methods because passive sampling can determine the rate of deposition of MPs within specific settings (location and time), whereas active sampling determines MPs in air masses(Rocha-Santos et al. 2022). Among 41 reviewed studies, only 6 papers used both active and passive sampling methods (Abbasi et al. 2019; Ding et al., 2021a; Dris et al. 2017; Ferrero et al. 2022; Kernchen et al. 2022; Yao et al., 2022).

In an experiment conducted by Ferrero et al., equipment was used to combine active and passive methods. This was characterized by a specific intake flow rate representing an active sampler, followed by a linear decrease in airspeed as a passive sampler(Ferrero et al. 2022).

3.1.4. Selection of sampling substrate

Airborne M/NPs are typically collected through samplers on inorganic or organic filters, with specific characteristics like pore size and composition depending on the analysis being performed later (Rocha-

Table 1
Summary of studies describing different pre-sampling procedures (sorted by the type of sampling).

paper	type of sampling	type of filter	pore/ diameter	air volume or air flow rate during active sampling	filter pretreatment
(Liu et al. 2019c)	active	glass (micro)fiber	1.6 μm / 90 mm	1,2,3,5,9,14,18, 30,72,100,144 m3	heating at 450 °C for 4 h prior to use
(O'Brien et al. 2020)	active	glass (micro)fiber	1.6 μm/-	55 m3/h	heating at 450 °C for 4 h prior to use.
(Wang et al. 2020)	active	glass (micro)fiber	1.6 μm / 90 mm	100 ± 0.1 L/min	heating at 450 °C for 4 h prior to use.
(Liu et al. 2019a)	active	glass (micro)fiber	1.6 μm/ 90 mm	100 ± 0.1 L/min	heating at 450 °C for 4 h prior to use and pre-examining microscopically each filter prior to use
(Vianello et al. 2019)	active	silver membranes	0.8 μm/ 20 mm (by tailoring 47 mm commercial filters)	0.82 L/min	flushing with nitrogen (N5.0) prior to use.
(González-Pleiter et al. 2021b)	active	stainless steel	25-μm /-		cleaning with Milli-Q water, wrapping with aluminum foil and heating to 300 °C for 4 h
(Peñalver et al. 2021)	active	glass fiber	-/150 mm	720 m3/day	heating at 450 °C for 4 h then weighing
(Wright et al. 2019)	active	quartz microfiber polytetrafluoroethylene mixed cellulose ester membrane alumina-based membrane silver membrane	2.2 μm /- 2.0 μm/- 0.8 μm/- 0.2 μm/- 1.2 μm/-	16.71 L/min	–
(Amato-Lourenço et al. 2022)	active	glass (micro)fiber	<1 μm/ 110 mm	3 L/min	weighing
(Xie et al. 2022)	active	alumina-based membrane	0.22 μm/16 mm	10 m3	–
(Rahman et al. 2021)	active	Teflon Teflon silver membrane	0.2 μm/ 37 mm 0.2 μm/ 47 mm 1.2 μm/37 mm	4 L/min 5 L/min 5 L/min	–
(Xu et al. 2020)	active	quartz microfiber	-/90 mm	–	–
(Liao et al. 2021)	active	glass (micro)fiber polytetrafluoroethylene (PTEF)	0.7 μm/ 90 mm 0.45 μm/ 47 mm	1 m3	heating at 450 °C for 4 h prior to use
(Chen et al. 2022)	active	Silver Whatman filter	0.2 μm/25 mm 0.45 μm/47 mm	8 L/min	–
(Trainic et al. 2020)	active	polycarbonate	0.8 μm/-	20 L/min	–
(Szewc et al. 2021b)	passive	glass (micro)fiber	1.6 μm/ 47 mm		heating at 500 °C for 8 h prior to use.
(Soltani et al., 2021a, 2021b)	passive	glass (micro)fiber	0.6 μm/ 9 cm		examining microscopically with X20 magnification and removing extraneous particles by rinsed forceps
(Klein and Fischer (2019))	passive	cellulose	5–13 μm/5 mm		–
(Abbasi & Turner 2021b)	passive	S&S filter papers	2 μm/-		
Huang et al., 2021)	passive	nitrocellulose	0.45 μm/ 47 mm		–
(Knobloch et al. 2021b)	passive	glass (micro)fiber	1.2 μm/47 mm		The equipment was pre-cleaned, three times with ultrapurewater (18 MΩ) and once with acetone before use.
(Finnegan et al., 2022)	passive				–
(Welsh et al. 2022)	passive	glass (micro)fiber	1.6 μm / 4.25 cm		
(Abbasi et al., 2022a)	passive	S&S filter papers	2 μm/ 150 mm		All equipment was triple rinsed with filtered B-pure™ or DI water prior to use
(Liu et al. 2022b)	passive	glass (micro)fiber	0.45 μm		heating at a high temperature
(Abbasi et al. 2022b)	passive	cellulose acetate membranes	1 μm/ -		–
(Dong et al. 2021)	passive	polycarbonate	0.45 μm/ 47 mm		all sampling tools were thoroughly cleaned with Milli-Q water
(Goßmann et al. 2022)	passive	glass fiber	1 μm/15 mm		heating at 400 °C for 4 h prior to use
(Wright et al. 2020)	passive	alumina-based membrane silver membrane	0.2 μm/- 1.2 μm/ -		–
(Liu et al. 2022b)	passive	glass (micro)fiber	1.0 μm/ -		heating at 500 °C for 3 h prior to their use
(Nematollahi et al. 2022)	passive	S&S filter papers	2 μm/ -		–

(*continued on next page*)

Table 1 (*continued*)

paper	type of sampling	type of filter	pore/ diameter	air volume or air flow rate during active sampling	filter pretreatment
(Abbasi et al. 2017)	passive	S&S filter papers	2 μm/ -		–
(Zhang et al. 2020)	passive	cellulose membranes	5 μm		–
(Cai et al. 2017)	passive	glass (micro)fiber	1 μm/-		–
(Abbasi et al., 2022c)	passive	S&S filter papers	2 μm/ -		–
(Ding et al. 2021b)	active & passive	glass (micro)fiber	3 μm / 90 mm	201–378 m3	heating at 450 °C for 4 h prior to use.
(Ferrero et al. 2022)	active & passive				cleaning with Milli-Q water and acetone prior to use
(Kernchen et al. 2022)	active & passive	aluminium oxide	0.2 μm/ 25 mm	0.6 m3	–
(Yao et al., 2022)	active & passive	quartz	2.2 μm/ 47 mm	The flowrate of 1.67 L/min for PM10 sample and 15 L/min for PM2.5 s	heating at 550 °C overnight prior to use
(Abbasi et al. 2019)	active & passive	polytetrafluoroethylene (PTFE) papers for active sampling S&S filter papers	2 μm/46.2 mm 2 μm/2 mm	16.67 L/mi for active sampling	–
(Dris et al. 2017)	active & passive	quartz	1.6 μm/ 47 mm	8 L/min for active sampling	–

Santos et al. 2022). However, there is no "one filter fits all" and various filter substrates such as cellulose, alumina, silver, and polycarbonate have been used and assessed. It is vital to select a filter that is not made of plastic materials as this can interfere with the chemical characterization. Moreover, For chemical identification, a low-interference substrate/filter is essential based on the analytical technique. While glass filters were used in 16 experiments, most of which had a pore size of 1.6 μm, 5 studies used silver filters, 3 of which had a 1.2 μm pore size, one used 0.2 μm, and the other one utilized a 0.8 μm pore size filter (Table 1). A nitrocellulose filter with a pore size of 0.45 μm was used in one study, while cellulose filters were used in another study. Alumina-based membrane filters with a 0.2 μm pore size were utilized in 3 studies. In addition, MPs were collected through S&S filter papers (Schleicher & Schuell filters with paper media) with 2 μm pore size and quartz filters with 2 μm pore size in 6 and 4 experiments respectively. Polytetrafluoroethylene (PTEF) and polycarbonate filters were also used for sampling in 3 and 2 studies, respectively.

3.2. Sampling strategy relevant for airborne M/NPs

Assessment of M/NPs has been performed by using particulate matter air samplers, through the collection of settling particles, collection from surfaces with brushes, breathing manikins, and air pumps. Detailed sampling protocols, such as describing the meteorological conditions, sampling locations (height of sampling), sampling equipment, and sampling duration are crucial for obtaining comparable data (GENERAL AIR SAMPLING GUIDELINES 1994; Rocha-Santos et al. 2022). However, only a limited number of studies have reported these aspects in their study.

3.2.1. Elevation of sampling

The height of sampling differs from one study to another depending on the scope and objective of the study. Studies conducted in an indoor environment used mainly 0.9–1.2 m height to simulate the human breathing height (Chen et al. 2022; Soltani et al., 2021a, 2021b; Vianello et al. 2019). In a study conducted by Liu K et al., although it was reported that sampling was performed at the height of 1.7 m which corresponds to the height that most people would be breathing in air, the considered human position (sitting or standing) was not mentioned. In addition, they utilized multiple heights (33, and 80 m) in outdoor settings for assessment of the sources, transportation, and potential ecological risk of MPs (Liu et al. 2019a). In outdoor experiments, various heights have been used, most of them were more than 10 m above the ground. However, studies at the height of 1.7 m, 1 m, and 3 m above the ground have been identified (Abbasi & Turner 2021a; Klein and Fischer, 2019; Liu et al. 2019a). In our review, an experiment conducted in 2021 was the only study that collected MPs directly from the atmosphere at a high altitude, averaging above the planetary boundary layer, which is 3500 m above sea level (a.s.L.) or ~ 2800 m above ground level (González-Pleiter et al., 2021).

3.2.2. Meteorological factors

As described in the (GENERAL AIR SAMPLING GUIDELINES 1994) meteorological parameters such as wind speed, wind direction, temperature, and humidity primarily affect the amount and distribution of a contaminant available in the air. Among all articles reviewed, only 16 recorded meteorological factors (Supplementary Table 2) and all of them assessed the wind speed and wind direction (Chen et al. 2022; Ding et al., 2021a; Dong et al. 2021; Ferrero et al. 2022; Huang et al., 2021; Kernchen et al. 2022; Liu et al. 2019b, a; Peñalver et al. 2021; Szewc et al. 2021a; Wang et al. 2020; Welsh et al. 2022; Wright et al. 2020). Their data indicates that the total amount of MPs was negatively associated with temperature and humidity (Amato-Lourenço et al. 2022). Besides the beforementioned meteorological factors, some studies assessed other factors including crosswind speed, headwind speed, wind chill temperature, dew point, psycho wet-bulb temperature, heat stress index, barometric pressure, station pressure, atmospheric pressure, and density altitude as meteorological factors (Wang et al. 2020; Wright et al. 2020). The positive correlation between barometric pressure and atmospheric MPs was illustrated by Liu et al(Liu et al. 2019b).

In indoor settings, the quality of ventilation is also essential for an accurate assessment of particle concentration. Interestingly, a study by Chen and colleagues measured indoor and outdoor CO_2, temperature, and relative humidity (RH) concentrations. They showed that CO_2 concentrations resulting from poorly ventilated nail salons were positively correlated with indoor MP concentrations, (Chen et al. 2022), which was in line with lower MP concentrations in a better-ventilated environment even with higher human activity levels or more plastic items within the environment (Xie et al. 2022).

3.3. Post-sampling

3.3.1. Storage and transport

After sampling, the filters must be sealed and transported to the laboratory and then stored for further analysis (Organization 1997). This step is not only essential for contamination avoidance but also

Table 2
Overview of the passive sampling method. (sorted by type of deposition).

Paper	type of deposition	sampler
(Ding et al., 2021a)	dry	funnel (d = 22 cm) & 2 L collection bottle
(Ferrero et al. 2022)	dry	Deposition box (50 × 50 × 20 cm^3 box covered by a pitched roof)
(Goßmann et al. 2022)	dry	spider web
(Abbasi et al. 2019)	dry	metallic pan and wooden brushy
(Abbasi et al. 2017)	dry	plastic dustpan and brush
(Dong et al. 2021)	wet	bucket
(Szewc et al. 2021b)	wet & dry	steel barrel, steel funnel (Ø 65 cm, 0.33 m^2), and 20 L glass jar
(Klein and Fischer (2019))	wet & dry	150 cm long PVC-pipe, a PE-funnel, and a 2 L PE-bottle.
(Abbasi & Turner 2021b)	wet & dry	customized metallic deposition collectors (diameter = 35 cm; area = 0.096 m^2)
(Huang et al., 2021)	wet & dry	22 L stainless steel bucket (diameter: 25 cm, height: 45 cm)
(Knobloch et al. 2021a)	wet & dry	a bottle with a funnel attached an open beaker a petri dish covered in double-sided adhesive tape an automatic wet deposition collector
(Kernchen et al. 2022)	wet & dry	stainless-steel funnel in glass bottles
(Welsh et al. 2022)	wet & dry	Bulk precipitation collectors: a square 0.25 m^2 collector with a stainless-steel, Teflon-coated funnel leading into a 50 L polyethylene carboy lined with two clear plastic bags. An 80-μm Nitrex nylon mesh filter was loosely inserted into the stainless-steel funnel (for insects or other contamination prevention) The wet-only precipitation collector: a battery-operated sampler comprised of a 0.0925 m2 collector, activated by moisture and automatically opened during precipitation periods. The precipitation passed through an-μm Nitrex nylon mesh filter and was collected in a carboy lined with two clear plastic bags.
(Abbasi et al. 2022b)	wet & dry	wet deposition: stainless steel spoon and 2-L glass jar dry deposition: metallic pot containing 500 mL of filtered, distilled water
(Wright et al. 2020)	wet & dry	aluminum rain gauge with a 0.03 m^2 (200 mm diameter) orifice
(Liu et al. 2022b)	wet & dry	stainless-steel funnel & 2.5 L glass bottle
(Cai et al. 2017)	wet & dry	a sampling device equipped with a glass bottle
(Soltani et al., 2021a, 2021b)	indoor deposition	glass Petri dishes (diameter = 12 cm)
(Nematollahi et al. 2022)	indoor deposition	brush made of horsetail strands and a steel dustpan
(Zhang et al. 2020)	indoor deposition	basin
(Dris et al., 2017)	indoor deposition	Quartz fiber
(Abbasi et al., 2022a)	indoor deposition	horse-hair brush and metal plate
(Abbasi et al., 2022b)	indoor deposition, wet & dry	wooden brush with horsehair bristles and a stainless steel dustpan
(Yao et al., 2022)	indoor deposition, wet & dry	indoor deposition: a quartz filter in a glass Petri dish and an empty glass Petri dish wet & dry deposition: four stainless steel funnels
(Liu et al. 2022b)	–	Pine needle

guarantees limited particle loss during sample transfer. There are several options for storage and transport but the most common are covering filters or the bottles where particles are collected and keeping them at a specific temperature. According to our review, 23 papers reported this step in their methodology, 7 of which used aluminum foil for covering filters or sampling jars (Abbasi et al., 2022a; Dong et al., 2021; Goßmann et al., 2022; Liu et al., 2022b,a; Yao et al., 2022; Abbasi et al., 2022b; Zhang et al., 2020). Four studies stored their filters in a pre-cleaned air sampling cassette (Ding et al., 2021a; Liao et al. 2021; Liu et al. 2019b; Wang et al. 2020) and covered them with aluminum foil, before being transported. In the reviewed studies, samples were stored at a controlled temperature of 23 ± 3 °C (Chen et al. 2022), 4 °C (Abbasi et al., 2022a; Dong et al., 2021; Kernchen et al., 2022; Abbasi et al., 2022b), −20 °C (Amato-Lourenço et al. 2022; Liu et al. 2022b) or after oven drying at 40 (Chen et al. 2022).

3.3.2. *Weighing filter substrate*

After collecting samples it is essential to take the necessary measures to ensure which of the following steps is the cause of potential particle loss. Weighing the filter on which particles have been collected (after sample collection and prior to any further procedure) is a way to document any loss of sample and has only been reported in 3 studies (Abbasi & Turner 2021a; Amato-Lourenço et al. 2022; Peñalver et al. 2021).

3.3.3. *Sample treatment and preparation*

Following collection, the next step is to separate M/NPs from any other matrix components present, such as organic and inorganic materials. This step aims to eliminate interference in the identification of M/NPs caused by organic, biogenic, and other non-plastic matter that might be present in the sampled particles. Numerous techniques are recommended for this purpose, including visual sorting, sieving, density separation, elutriation, flotation, digestion, and enzymatic digestion (Rocha-Santos et al. 2022).

Treatment In this review, 21 papers reported treatment procedures including oxidation (19 studies), density separation (11 studies), and sieving and filtration (6 studies), for details see Table 4. However, it is noteworthy that the sample treatment procedures (digestion and flotation) were excluded in 2 studies in order to reduce the loss of particles or MP contamination during the many steps (Soltani et al., 2021a, 2021b; Zhang et al. 2020).

To remove organic matter by the oxidation process, 15 papers used only H_2O_2 (30% w/w solution) while 2 papers used Fenton's reagent (H_2O_2 and $FeSO_4$). In addition, 8 studies treated samples with $ZnCl_2$ and 2 studies used NaI, and another study NaBr for density separation; 5 studies used sieving along with either oxidation or density separation for their sample treatment; and one used enzymatic digestion with the aid of sodium dodecyl sulfate (SDS), protease, cellulase, and chitinase enzymes. Three studies used 3 different steps including sieving, oxidation, and density separation for the treatment procedure (Abbasi et al., 2017, 2022a; Nematollahi et al., 2022) (Fig. 2) (Table 4).

Preparation Following the treatment steps, samples are prepared for analysis in order to provide analytical information regarding the characteristics and M/NP concentration. Typically, sample preparation is performed in experiments with a passive sampling methodology. In particular, 16 studies performed a washing step using ultrapure water in order to rinse the glass after passive sampling to minimize the adhesion of particles to the internal walls of the container. Subsequently, the suspension was vacuum-filtered through a filter for further analysis (Abbasi et al., 2019, 2022a,c; Abbasi and Turner, 2021a; Dong et al., 2021; Goßmann et al., 2022; Huang et al., 2021; Klein and Fischer, 2019; Knobloch et al., 2021a; Liu et al., 2022b; Nematollahi et al., 2022; Soltani et al., 2021a,b; Szewc et al., 2021a; Welsh et al., 2022; Wright et al., 2020; Abbasi et al., 2022b). Moreover, in 2 passive sampling experiments, particles were transferred onto a calcium fluoride(CaF_2) substrate with the aim of acquiring a better spectrum for analysis,

Table 3
Overview of active sampling and considerable parameters (sorted by the type of sampler).

Paper	type of sampler	sampling flow rate (m3 or L/time)	run time	volume of air sampled (m3)
(Liu et al. 2019b)	KB-120F particulate sampler		continuously	1,2,3,5,9,14,18,30,72,100,14
(Wang et al. 2020)	KB-120F type intelligent middle flow total suspended atmospheric particulate sampler	100 ± 0.1 L/min	10–48 h	53–259 per sample
(Liu et al. 2019a)	KB-120F type intelligent middle flow total suspended particulate sampler	100 ± 0.1 L/min	1 h	6 of air per sample
(Xu et al. 2020)	The intelligent total suspended particulate (TSP) comprehensive sampler			
(O'Brien et al. 2020)	high volume total suspended particle air sampler	55 m3/h	19 min	
(Liao et al. 2021)	LB-120F intelligent middle flow total suspended particulate sampler	100 ± 0.1 L/min	between 10 AM-4 PM	1
(Rahman et al. 2021)	Harvard cascade impactors	5 L/min	7 days	
(Rahman et al. 2021)	Harvard cascade impactors	5 L/min	96 h	
(Kernchen et al. 2022)	A custom-built pump with a nominal volume flow rate of 9 L min − 1 powered with a Li-ion battery pack	3.4 L min − 1	3 h	0.6
(Dris et al. 2017)	A pump (Stand-alone sampling pump GH300)	8 L/min	4–7 h for indoor 10–40 h for outdoor	2–5 for indoor 5–20 for outdoor
(Ding et al., 2021a)	Tisch TE-1000 PUF			201–378
(Vianello et al. 2019)	Breathing Thermal Manikin	0.82 L/min	24 h	16.8
(Peñalver et al. 2021)	DIGITEL DHA 80 sampler equipped with a PM10 inlet	720 m3/day	24 h	
(Wright et al. 2019)	Partisol 2025 Sequential Air Sampler	16.7 L/min	4 h	
(Yao et al., 2022)	Thermo Scientific™ Partisol™ 2000i-D Dichotomous Air Sampler	1.67 L/min for PM10 sample and 15 L/min for PM2.5 s		
(Rahman et al. 2021)	OMNI FT ambient air samplers PM2.5 impactors	5 L/min	7 days	
(Abbasi et al. 2019)	ECHO PM ambient filter sampler	16.67 L min-1	24 h	
(Amato-Lourenço et al. 2022)	a Handi-vol sampler	3 L/min	24 h	
(Ferrero et al. 2022)	Deposition Box	1.5 m3/h	continuously	
(Xie et al. 2022)	filter flasks were connected by a rubber tube and a long-neck funnel was used for the suction of air connected to an active air sampler	2.5 m3/h	4 h	10
(Rahman et al. 2021)	personal environmental monitor	4 L/min	24 h	
(Chen et al. 2022)	25 mm Cassettes	9 L/min	8 h	5.43 for indoor 5.08 for outdoor
(Trainic et al. 2020)	a funnel connected with conductive tubing (1.9 cm inner diameter) to filter holders	20 L/min		12–60

although the details of this step were not provided by the authors (Kernchen et al. 2022; Knobloch et al. 2021a). Interestingly, in a passive sampling study conducted by (Wright et al. 2020), samples were transferred from an aluminum membrane filter to a silver membrane immediately after the sampling step and with skipping the treatment step. (Wright et al. 2020). In an experiment conducted by (Klein and Fischer, 2019), particles were collected from cellulose filters with the aid of a tweezer and transferred to slides for polymer identification by Raman. (Abbasi et al., 2022a) attached their collected particle to microscope slides via double-sided adhesive tape.

M/NPs collected by active sampling on the filter are usually not extracted but are rather investigated directly on the filter (Amato-Lourenço et al. 2022; Liu et al. 2022b; O'Brien et al. 2020; Wang et al. 2020; Wright et al. 2019)(Fig. 2). However, 5 studies used preparatory steps to transfer particles to a more suitable substrate such as Zinc selenide (ZnSe), Calcium fluoride (CaF2), and Klarite to obtain accurate results from analytical methods(Chen et al. 2022; Liao et al. 2021; Rahman et al. 2021; Vianello et al. 2019; Xu et al. 2020). In two of these studies, the samples were first treated before being transferred(Chen et al. 2022; Luo et al. 2020).

Another preparatory step performed in 2 experiments, is to compress and flatten samples (in this case MPs) to an ideal thickness for such analyses, specifically FTIR, which is discussed in section 4.2.1. (Finnegan et al., 2022; Zhang et al. 2020). (Finnegan et al., 2022) pressed fibers by 13 mm diameter stainless steel die-pellets. However, Zhang and colleagues picked out particles with tweezers and placed them on the micro compression cell with a diamond window to compress them to a uniform thickness for IR measurements (Zhang et al. 2020).

3.4. Analysis

3.4.1. Visual analysis

The characteristics of MPs are a vital step which in turn demonstrates their distribution and impact on the environment (Rocha-Santos et al. 2022). Physical characteristics of atmospheric MPs such as shape, size, color, and number are observed and counted through various types of microscopes. According to the aim of the study, different microscopes for visual analysis are used. Based on our review, the stereomicroscope is the most commonly used device for the physical characterization of airborne MPs, which was used in 13 experiments (Supplementary

Table 4
Summary of the treatment procedure (sorted by type of sampling).

paper	type of sampling	matrix	oxidation	density separation	sieving	enzymatic digestion	details
(Xie et al. 2022)	active	air	✓				removing calcium carbonate with sodium hypochlorite solution (NaClO) dilute at a final pH of 3 for 24 h
(Rahman et al. 2021)	active	air	✓				oxidation with 30% w/w H2O2 for 48 h
(Xu et al. 2020)	active	air	✓				oxidation with 30% w/w H2O2
(Liao et al. 2021)	active	air	✓				oxidation with 30% w/w H2O2
(Dris et al. 2017)	active	air		✓	✓		sieving through a 2.5-mm mesh
(Chen et al. 2022)	active	air	✓	✓			density separation with ZnCl2 oxidation with 30% w/w H2O2 for 6 days and density separation with ZnCl2
(Klein and Fischer (2019))	passive	rainwater	✓				removing calcium carbonate with sodium hypochlorite solution (NaClO, 6–14%) for 24 h
(Abbasi & Turner 2021b)	passive	settled dust	✓	✓			oxidation with 30% w/w H2O2 and density separation with a solution of ZnCl2
(Huang et al., 2021)	passive	rainwater	✓				oxidation with 30% w/w H2O2 for 24 h at room temperature
(Kernchen et al. 2022)	passive	rain water	✓		✓	✓	filtration through 500 μm and 5 μm stainless steel filters, oxidation with Fenton's reagent (FeSO4 + H2O2), and enzymatic digestion with SDS, protease, cellulase digestion, and chitinase
(Abbasi et al., 2022a)	passive	settled dust	✓	✓	✓		sieving through a 5-mm stainless steel mesh oxidation with 30% w/w H2O2 and density separation with a solution of ZnCl2
(Yao et al., 2022)	passive	rainwater	✓				oxidation with 30% w/w H2O2
(Liu et al. 2022b)	passive	air	✓	✓			density separation with NaBr and oxidation with 30% H2O2 for digestion
(Abbasi et al. 2022b)	passive	water (snow)	✓	✓			density separation with ZnCl2 and oxidation with 30% w/w H2O2 for 12 h
(Dong et al. 2021)	passive	rain water	✓		✓		filtration through a 50 μm stainless-steel mesh (mesh size: 50 μm) and oxidation with 30% (v/v) H2O2
(Goßmann et al. 2022)	passive	air	✓				oxidation with Fenton's reagent (FeSO4 + H2O2)
(Liu et al. 2022b)	passive	rainwater		✓			density separation with ZnCl2
(Abbasi et al. 2019)	passive	settled dust	✓	✓			oxidation with 30% H2O2 for 8 days density separation with NaI
(Nematollahi et al. 2022)	passive	settled dust	✓	✓	✓		sieving through a 5-mm metal mesh oxidation with 30% w/w H2O2 for 10 days and density separation with ZnCl2
(Abbasi et al. 2017)	passive	settled dust	✓	✓	✓		sieving through a 5-mm mesh oxidation with 30% w/w H2O2 for 7 days and density separation with NaI

Table 3). Fluorescence microscopy was also used in 7 studies, 4 of which described Nile Red staining as a preparation step for visual observation of MPs (Amato-Lourenço et al. 2022; Klein and Fischer, 2019; Liao et al. 2021; Wright et al. 2020). This step was performed by adding Nile Red solution to the filters and letting them get dry at room temperature. Moreover, 7 studies determined the morphology of M/NPs by utilizing a scanning electron microscope (SEM), binocular microscopy (8 studies), and polarized light microscopy (PLM) (3 studies). MPs are non-conductive material samples and therefore require a coating for SEM analysis, these coatings are typically carbon and/or metal such as gold (Au), gold/palladium (Au/Pd), platinum (Pt), silver (Ag), chromium (Cr) or iridium (Ir) as described in 4 studies (Abbasi et al., 2019, 2022a; Nematollahi et al., 2022; Yao et al., 2022; Abbasi et al., 2022b). In 3 studies both techniques, binocular microscope and SEM, were applied (Abbasi et al. 2022b; Abbasi et al., 2022c; Nematollahi et al. 2022). (Abbasi et al. 2017, 2019) applied four different microscopy methods including binocular, fluorescence, polarized light, and scanning electron microscope. In 5 experiments, the type of microscope used to determine color, and size was not specified (Cai et al. 2017; Chen et al. 2022; Nematollahi et al. 2022; O'Brien et al. 2020). Interestingly, in 5 experiments MPs were visually assessed by a microscope coupled to Raman or FTIR for chemical characterization, which is discussed in later sections (Kernchen et al. 2022; Liu et al. 2022b; Vianello et al. 2019; Xu et al. 2020; Yao et al., 2022).

3.4.2. Limit of detection

In general, the limit of detection (LOD) is the lowest possible unit (size/concentration) at which the method can detect within the matrix with a certain degree of confidence (Rousseau 2001). Based on the collected data, 15 papers reported LOD for different types of microscopes. The lower size limit for the stereomicroscope was reported as 50 μm (Dong et al. 2021; Soltani et al., 2021a, 2021b; Welsh et al. 2022), 20 μm (Knobloch et al. 2021b), and 12.5 μm (Huang et al., 2021). In addition in experiments that used fluorescence microscopy 50 μm (Amato-Lourenço et al. 2022), and 5 μm (Liao et al. 2021) were recorded as the LOD. The LOD was approximately 20 nm for the scanning electron microscope. In studies that used a binocular microscope, the LOD was reported as 12 μm (Amato-Lourenço et al. 2022), 20–50 μm (Abbasi

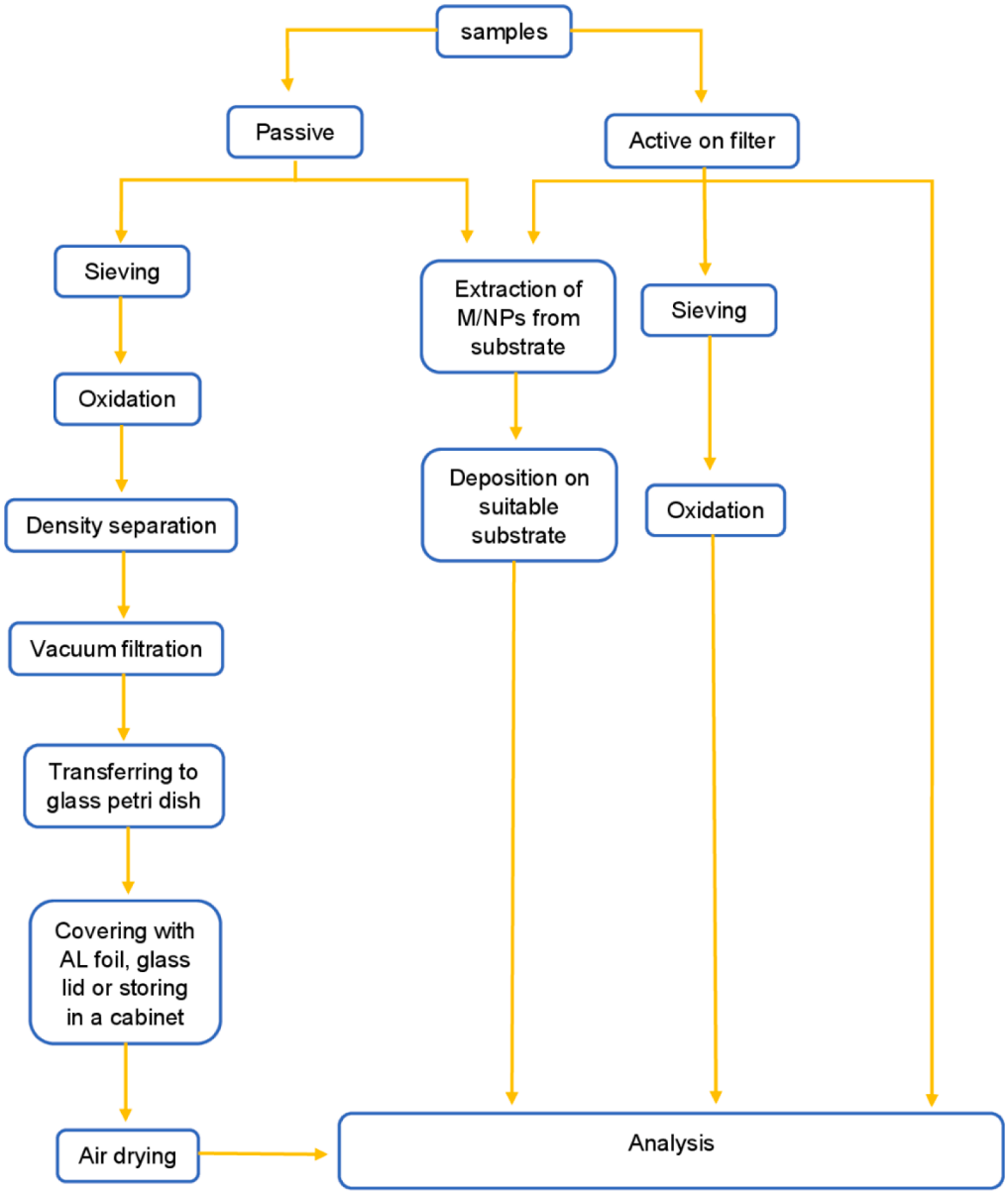

Fig. 2. General overview of sample preparation steps for MPs in passive and active sampling method.

et al., 2022c), 30–50 μm (Abbasi et al., 2022a), and 1 μm (Xie et al. 2022).

3.4.3. Criteria for visual screening of MPs

In order to separate and identify the plastics from other materials such as metal, paint coatings, tar, glass, etc., visual sorting is essential. In particular, certain criteria are used that ensure correct identification and prevent misidentification and underestimation of M/NPs (Ding et al., 2021a). In our review, 17 out of 41 experiments used criteria for considering suspect particles as MPs. The technique used to identify atmospheric MPs varies depending on the weathering effect and particle size. However, the following guidelines are mainly used in reviewed articles (Abbasi et al., 2017, 2019, 2022a,c; Abbasi and Turner, 2021a; Ding et al., 2021; Huang et al., 2021; Klein and Fischer, 2019; Liu et al., 2022b; Abbasi et al., 2022b; Amato-Lourenço et al., 2022):

(1) homogeneous and clear colors (used in 12/17 studies);
(2) no organic or cellular structures should be visible (used in 13/17 studies);
(3) shiny or glossy appearance (used in 8/17 studies);
(4) fibers should be equally thick throughout their entire length and should not be entirely straight (used in 12/17 studies).

Along with the aforementioned criteria, the hardness and elastic properties of particles were analyzed in 6 experiments using tweezers to identify plastic particles (Abbasi et al., 2017, 2019, 2022a,c; Abbasi and Turner, 2021a; Welsh et al., 2022; Abbasi et al., 2022b). In 2 separate experiments conducted in 2022 and 2017, reaction to a hot stainless steel needle was used as an identification criterion (Abbasi et al., 2022a-c). In contrast to the third criterion above, non-shiny particles were included as MPs by Klein and Fischer (Klein and Fischer, 2019). Moreover, particles that were colored unnaturally under bright-field compared to the rest of the sample were used as identification criteria in 2 studies (Welsh et al. 2022; Wright et al. 2020). In addition, transparent or white particles must be examined under high magnification and a fluorescence microscope (Abbasi et al. 2017, 2019; Amato-Lourenço et al. 2022).

3.4.4. Physical assessment

After visual identification, the quantity, shape, size, and color of the

observed MPs are analyzed.

Shape: Plastic debris is commonly categorized based on its shape as spheres or beads, foams, fibers, fragments, and films. By their definition, microbeads are spherical particles with every point on their surface having the same distance from its center while fragments are debris and have an irregular shape with 3 dimensions having a length-to-width ratio of < 3 (Soltani et al., 2021a, 2021b; Vianello et al. 2019; Yao et al., 2022); fibers are cylindrical or slender long lines (aspect ratio of 3 or more) (Liao et al. 2021; Vianello et al. 2019; Xie et al. 2022) of equal thickness and in most studies fibers are not considered straight (Abbasi et al., 2022c; Ferrero et al. 2022; Klein and Fischer, 2019); films (or sheets) are defined as "2-dimensional' shapes (Soltani et al., 2021a, 2021b) or slice thinner than fragments (Dong et al. 2021; Wright et al. 2020; Yao et al., 2022); and foams have a sponge-like texture (Abbasi et al. 2017; Soltani et al., 2021a, 2021b). Based on our review, 37 papers assessed and categorized MPs by their shape. Fibers were identified in all of them except for a study conducted by (Rahman et al. 2021) (Table 5). Two studies aimed to collect and analyze fibers only (Finnegan et al., 2022; O'Brien et al. 2020). Thirty one studies identified fragment-shaped particles while microbeads, foam, and films were observed in 15, 5, and 16 studies, respectively. In addition in a study conducted by (Rahman et al. 2021)**Error! Reference source not found.** Powder-shaped MPs were also reported as a morphological structure. Along with MPs, MRs were also categorized into sheet-like layers, fibers, or fragments in 2 studies and in both of them fragments were the most dominant one (Table 6) (Abbasi et al. 2017, 2019).

Depending on the type of sampling, the major shapes of MPs identified by passive sampling were fibers, while the predominant shape identified by active sampling was fragments. Based on the experimental setting (Table 5), fibers were identified as the predominant shape in 19

Table 5
Shapes of airborne microplastics in reviewed studies (sorted by the type of environment).

paper	environment	type of sampling	characteristic	fibers	fragments	microbead	foam	powder	film
(Liu et al. 2019c)	outdoor	active	urban	✓	✓*	✓			
(Wang et al. 2020)	outdoor	active	remote (over the ocean)	✓*	✓				
(Ding et al. 2021b)	outdoor	active & passive	remote (above the sea)	✓*	✓	✓	✓		✓
(Liu et al. 2019a)	outdoor	active	urban	✓*	✓	✓			
(Klein and Fischer (2019))	outdoor	passive	urban & rural	✓	✓*				
(González-Pleiter et al. 2021b)	outdoor	active	rural, sub rural, low density urban and high-density urban	✓ *sub rural & rural	✓ *urban				
(Abbasi & Turner 2021b)	outdoor	passive	urban & remote (mountain)	✓*					
(Huang et al., 2021)	outdoor	passive	urban	✓*	✓	✓			✓
(Knobloch et al. 2021b)	outdoor	passive	suburban	✓*	✓	✓			✓
(Finnegan et al., 2022)	outdoor	passive	not specified	✓*					
(Ferrero et al. 2022)	outdoor	active & passive	(remote) over the sea	✓*	✓				
(Kernchen et al. 2022)	outdoor	active & passive	rural, suburban, and urban	✓	✓*	✓			
(Amato-Lourenço et al. 2022)	outdoor	active	urban	✓*					
(Welsh et al. 2022)	outdoor	passive	country	✓*	✓				
(Abbasi et al., 2022a)	outdoor	passive	urban	✓*	✓	✓			✓
(Liu et al. 2022b)	outdoor	passive	urban	✓	✓*				✓
(Abbasi et al. 2022b)	outdoor	passive	urban	✓*	✓	✓			✓
(Dong et al. 2021)	outdoor	passive	lake	✓*	✓	✓	✓		✓
(Goßmann et al. 2022)	outdoor	passive	urban	✓*					
(Wright et al. 2020)	outdoor	passive	urban	✓	✓*	✓	✓		✓
(Liu et al. 2022b)	outdoor	passive	urban	✓*	✓		✓		✓
(Abbasi et al. 2019)	outdoor	active & passive	urban & industrial	✓	✓	✓*			✓
(Abbasi et al. 2017)	outdoor	passive	urban & industrial	✓*	✓	✓			✓
(Szewc et al. 2021b)	outdoor	passive	urban	✓*	✓				
(O'Brien et al. 2020)	indoor	active		✓*					
(Vianello et al. 2019)	indoor	active		✓	✓*				
(Soltani et al., 2021a, 2021b)	indoor	passive		✓*	✓				✓
(Nematollahi et al. 2022)	indoor	passive	urban	✓*	✓				✓
(Zhang et al. 2020)	indoor	passive		✓*	✓				
(Cai et al. 2017)	indoor	passive		✓*	✓		✓		✓
(Abbasi et al., 2022a)	indoor	passive	urban	✓*	✓	✓			✓
(Yao et al., 2022)	indoor & outdoor	active & passive	not specified	✓	✓*				✓
(Xie et al. 2022)	indoor & outdoor	active	urban	✓	✓*	✓			
(Rahman et al. 2021)	indoor & outdoor	active	not specified		✓	✓		✓	
(Liao et al. 2021)	indoor & outdoor	active	urban & rural	✓	✓*				
(Dris et al. 2017)	indoor & outdoor	active & passive	around city	✓*					
(Chen et al. 2022)	indoor & outdoor	active	urban	✓	✓*				

* dominants shapes.

Table 6
Shapes of airborne micro rubbers in reviewed studies.

paper	fiber	fragment	spherule	film like	environment	characteristic	matrix
(Abbasi et al. 2019)	✓	✓*dust and air	✓	✓	outdoor	urban & industrial	air & settled dust
(Abbasi et al. 2017)	✓	✓*		✓	outdoor	urban & industrial	settled dust

outdoor and 5 indoor experiments, while 6 outdoor experiments showed fragments as the prevalent shape, and in one outdoor study microbeads were the major shape of particles identified. Based on the characteristic of the sampling area, fibers were predominantly identified in 11 urban sites. In an experiment analyzing both indoor and outdoor environments, it was illustrated that although the predominant shape of MPs was fragment, among outdoor environments, fibers were the prevalent shapes of MPs in the urbanized situation in comparison to rural areas (Liao et al. 2021). In an investigation done by (González-Pleiter et al., 2021), the dominant shapes of particles in urban and non-urban environments were respectively fragments and fibers. However, in the studies done by (Kernchen et al. 2022) and (Klein and Fischer, 2019) the predominant shape of particles in each type of characteristic (urban, rural, sub-rural, etc.) was not specified.

Size: Size is the most commonly used criterion to categorize microplastics. The minimum size of the collected microplastics directly depends on the sampling and processing methods(Rocha-Santos et al. 2022). According to our review, 34 papers assessed and reported suspected MPs size. Different size ranges have been described for particles depending on the size limit and pore size of the filters, the method of sampling used for collecting, and the setting of studies (Table 7). In our review, the majority of particles had a size range of 50–5000 μm, with each paper having its size range (Table 7) (Abbasi et al., 2017, 2022a; Klein and Fischer, 2019; Knobloch et al., 2021a; Abbasi et al., 2022b). While in 12 studies the lowest detected MPs were smaller than 50 μm, in 2 studies the smallest MPs sample observed were around 2–3 μm and < 1 μm, respectively (Rahman et al. 2021; Yao et al., 2022). Interestingly, (Rahman et al. 2021) detected particles in the nanometer range size which were reported as particles smaller than 1 μm. According to the filter's pore size, NPs (<1 μm) were collected through Teflon and silver filters with 0.2 μm and 1.2 μm pore sizes, respectively. However, size measurement was performed after transferring samples onto a CaF_2 because it was difficult to observe particles on filters. (Szewc et al. 2021a) reported that the smallest particle identified by 1.6 μm pore size was 5 μm. Based on the sampling method, particles larger than 12 μm were mostly observed during active sampling. When the passive sampling method was used, mainly MPs smaller than 100 μm were observed (Table 7).

In addition, Given the setting of the study, (Dris et al. 2017) and (Xie et al. 2022) showed that on average indoor MPs are larger than outdoor MPs. The size distribution of the MPs was also assessed at different heights and showed that the largest particles, including 9955 μm, 504.6 μm, and 2230 μm were found at 1.7 m, 33 m, and 80 m above the ground, respectively (Liu et al. 2019a).

Furthermore, the size of the MRs was also assessed in 2 separate experiments performed by Abbasi et al., 2019, 2017. They reported that based on the length of the MRs, a size range between ≤ 100 μm and L ≤ 1000 μm was reported, with the highest percentage of MRs encountered in the 100–250 μm size range (Abbasi et al. 2017, 2019).

Among the papers that performed particle size analysis, only 23 studies explained the procedure, software, or instrument used for the measurement (Table 7). Fifteen studies used the Image J software coupled with microscopy for size measurements. Although the majority of studies using ImageJ did not provide details on the measurement procedure, (Xie et al. 2022) provided some details and further explanations on the 2D size determination, and two other experiments reported that size measurements were performed along the largest dimension of MPs (Nematollahi et al. 2022; Wang et al. 2020). Moreover, to determine the particle size, the method of converting the number of pixels into a known length in millimeters was applied (Welsh et al. 2022). In a study by (Vianello et al. 2019), the MP hunter program (software was developed at Aalborg University (AAU) in collaboration with Alfred Wegener Institute (AWI)) was used in conjunction with μFTIR- image analysis for particle size measurement. In particular, the major dimension of a particle was calculated by finding the longest distance between the pixels of the particle. (Huang et al., 2021) were the only ones to use an eyepiece micrometer for particle size measurement.

Color: By categorizing plastic debris according to color, it is possible to identify potential sources (Abbasi et al., 2022a; Dong et al., 2021; Liu et al., 2019; Abbasi et al., 2022b). In this review, 27 papers analyzed inspected particles to determine the color pattern. Most reported colors are white, pink, black, red, yellow, gray, blue, green, transparent, purple, orange, brown, and indigo (Table S4). 'Clear color' has also been described as a group for classification in 3 investigations (Finnegan et al., 2022; Knobloch et al. 2021a; Welsh et al. 2022). In addition, in 7 experiments, MPs were classified into several color spectra such as black-grey, blue-green, red-pink, yellow-orange, and white-transparent, and in 4 of them, the white-transparent group was identified as a dominant color (Abbasi et al., 2017, 2019, 2022a,c; Huang et al., 2021; Nematollahi et al., 2022; Abbasi et al., 2022b). According to our results, blue was the most commonly observed color, followed by black and red overall. In the study working on MRs, black was the only observed color (Abbasi et al. 2017, 2019).

Surface morphology: Seven studies assessed the topography of airborne M/NPs, 5 of which collected their samples from settled dust, 1 study from the air and settled dust, 1 study from air and rainwater, and 1 study from the snow. The results show that 2 studies observed smooth surfaces(Abbasi et al. 2022b; Nematollahi et al. 2022) and others observed irregular surfaces(Abbasi et al., 2017, 2019, 2022a; Yao et al., 2022; Abbasi et al., 2022b).

3.4.5. *Chemical analysis*

Following physical characterization, airborne M/NPs are further analyzed for their chemical compositions. The chemical characterization of MPs is essential to differentiate between plastics and other particles. It also allows discovering their sources, exploring the degree of weathering, and determining which chemical additives are associated with the MP(Kershaw et al. 2019). Based on our review, 36 papers identified the chemical composition of MPs. The predominant polymers were polyethylene (PE), polypropylene (PP), polyamide (PA) or nylon, polystyrene (PS), polyethylene terephthalate (PET), polyester (PEST), and polyvinyl chloride (PVC). Various techniques are applied to obtain the chemical composition of M/NPs, including spectroscopic analysis such as infrared or Raman spectroscopy, allowing characterization without destruction of the sample (Renner et al. 2019). Chromatographic techniques are proven to determine the composition of environmental samples without the need for complex sample preparation such as thermal extraction, desorption gas chromatography, and Pyr-GC–MS (Dümichen et al. 2017; Kershaw et al. 2019) to provide multi-component results.

3.4.6. *Fourier transformed Infra-Red (FTIR)*

Synthetic polymers can be identified based on their highly specific IR spectra and distinct spectral bands via FT-IR spectroscopy (more details in the supplementary material. Text S1) (Bhargava et al. 2003). In our review, 23 studies utilized FTIR analysis for polymer identification in MPs (Table 8). In addition, FTIR instruments are often combined with a microscope allowing visualization and measuring of particles and it is

Table 7
Measurement methods and size ranges of atmospheric plastic particles in reviewed studies (sorted by the type of environment).

paper	environment	matrix	type of sampling	filter pore size	range	size limit	method of measurement
(Liu et al. 2019c)	outdoor	air	active	1.6 μm	12.35–2191.32 μm		
(Wang et al. 2020)	outdoor	air	active	1.6 μm	58.59 μm – 2251.54 μm		microscope coupled with ImageJ software along their largest dimension
(Ding et al. 2021b)	outdoor	air	active & passive	3 μm	50 μm – 2210 μm		
(Liu et al. 2019a)	outdoor	air	active	1.6 μm	23.07 μm – 9555 μm		
(Klein and Fischer (2019))	outdoor	rainwater	passive		>300 μm, 300–63 μm and <63 μm		
(González-Pleiter et al. 2021b)	outdoor	air	active		<30 μm – 5000 μm	25 μm	microscope Euromex-Edublue equipped with USB digital camera and ImageFocus 5
(Abbasi & Turner 2021b)	outdoor	settled dust & rainwater	passive	2 μm	<100 μm –1000 > μm	20 μm	microscope coupled with ImageJ software
(Huang et al., 2021)	outdoor	rainwater	passive	0.45 μm	<50 μm – 4–5 mm	12.5 μm	eyepiece micrometer (S-EYE)
(Knobloch et al. 2021b)	outdoor	air	passive	1.2 μm	<200 μm – 500 > μm	20 μm	
(Ferrero et al. 2022)	outdoor	air	active & passive		not specified (*fiber length median 427 ± 59 μm and fiber width median and 17 ± 2 μm)		stereomicroscope embedded in the Renishaw™ μ-Raman coupled with a camera Length and width were measured using the segmented line tools, and straight-line tools respectively. The width was measured in three random points and then an average width was calculated.
(Kernchen et al. 2022)	outdoor	air & rainwater	active & passive	0.2 μm	11 μm-2000 μm		
(Amato-Lourenço et al. 2022)	outdoor	air	active	<1 μm	fiber length: 50.01 μm – 1579.43 μm particles diameter: 50.12 μm – 877.09 μm	50 μm	microscope coupled with ImageJ software fibers length and particles diameter
(Welsh et al. 2022)	outdoor	rainwater	passive	1.6 μm	20 μm – 4500 μm		microscope coupled with ImageJ software by converting the number of pixels measured to a known length in millimeters
(Abbasi et al., 2022a)	outdoor	settled dust	passive	2 μm	< 100 μm - ≥ 1000 μm	Microsocpe:20–50 μm SEM: 20 nm	microscope coupled with ImageJ software
(Liu et al. 2022b)	outdoor	air	passive	0.45 μm	<5 μm – 5000 μm		microscope coupled with ImageJ software
(Abbasi et al. 2022b)	outdoor	water (snow)	passive	1 μm	<100 μm - ≥1000 μm		microscope coupled with ImageJ software
(Dong et al. 2021)	outdoor	rainwater	passive		5 μm – 5000 μm		
(Wright et al. 2020)	outdoor	rainwater	passive	alumina-based membrane: 0.2 μm silver membrane: 1.2 μm	fiber diameter: 5 μm – 75 μm fiber length: <100 μm-≥3000 μm non-fibrous: 25 μm-≥350 μm		microscope coupled with ImageJ software
(Liu et al. 2022b)	outdoor	air & rainwater	passive	1.0 μm	50 μm –5000 μm		microscope coupled with image analysis software (Olympus stream)
(Abbasi et al. 2019)	outdoor	air & settled dust	active & passive	2 μm	≤ 100 μm –5000 μm	2 μm	microscope coupled with ImageJ software

(*continued on next page*)

Table 7 (*continued*)

paper	environment	matrix	type of sampling	filter pore size	range	size limit	method of measurement
							in terms of length or primary diameter
(Abbasi et al. 2017)	outdoor	settled dust	passive		≤ 100 μm −5000 μm		
(Szewc et al. 2021b)	outdoor	air/ rainwater	passive	1.6 μm	5 μm − 5000 μm		microscope camera software NIS Elements Basic Research
(Yao et al., 2022)	indoor & outdoor	air & rainwater	active & passive	2.2 μm	2 μm –3 μm	Raman microscope: 1 μm	
(Xie et al. 2022)	indoor & outdoor	air	active	0.22 μm	2.40 μm–2181.48 μm in longest dimensionn	larger than 1 μm	microscope coupled with ImageJ software
							in two dimensions
(Rahman et al. 2021)	indoor & outdoor	air	active	Teflon: 0.2 μm Silver:1.2 μm	MP < 1 μm	30 to 50 μm	
(Liao et al. 2021)	indoor & outdoor	air	active	0.7 μm	5 μm − 5000 μm	larger than 5 μm	microscope coupled with ImageJ software
(Dris et al. 2017)	indoor & outdoor	air	active & passive	1.6 μm	50 μm − 4850 μm	50 μm	microscope coupled with ImageJ software with the software Histolab®
							via their length
(Chen et al. 2022)	indoor & outdoor	air	active		<50 μm −200 μm< * (the 25 to 50 μm MPs are presented as < 50 μm)	25 μm	
(O'Brien et al. 2020)	indoor	air	active	1.6 μm	19 μm − 3948 μm		length of fibers via microscope coupled with a Motic Images
							Plus
(Vianello et al. 2019)	indoor	air	active	0.8 μm	11 μm − 50 μm	The size limits were adapted	MPhunter based on
							the μFTIR-Imaging analysis
						to 11 μm for the major dimension and 5.5 μm for the minor dimension	
(Soltani et al., 2021a, 2021b)	indoor	air	passive	0.6 mm	50 μm − 5000 μm	Microscopic lengths of 50 μm for fibers were defined as the lower size limit	microscope equipped with a Motic
							1080 camera and Motic Image Plus 3.0 software
(Nematollahi et al. 2022)	indoor	settled dust	passive	2 μm	50 μm −5000 μm		microscope coupled with ImageJ software
							the length of the largest aspect of the MP
(Zhang et al. 2020)	indoor	air	passive	5 μm	not specified	50 μm	microscope coupled with ImageJ software
					(*50 μm − 2000 μm for the majority of MPs)		
(Abbasi et al., 2022a)	indoor	settled dust	passive	2 μm	<100 μm −1000 > μm	30–50 μm	microscope coupled with ImageJ software

called micro-FTIR (μFT-IR) which has been performed in 19 studies reviewed.

Substrate In order to achieve an optimal result, the substrates used for analysis must have low IR interference (Käppler et al. 2015). Based on our review, MPs were directly analyzed on filters on which they were collected, including glass (micro) fiber filters in 9 studies (Amato-Lourenço et al. 2022; Ding et al., 2021a; Liao et al. 2021; Liu et al. 2019b, a; Liu et al. 2022b; Wang et al. 2020), nitrocellulose membrane filter (Zhang et al. 2020), silver membrane filter (Wright et al. 2020), and quartz filter (Dris et al. 2017). Other studies have used a method which involves the transfer of particles to a substrate suitable for FTIR analysis. In a study conducted by (Vianello et al. 2019), particles were transferred from silver membrane filters to a zinc selenide (ZnSe) window for FTIR analysis. Other possible types of slides for FTIR analysis included calcium fluoride (CaF_2) slides, used in 2 studies (Kernchen et al. 2022; Knobloch et al. 2021a), gold-coated slides, also used in 2 studies (Finnegan et al., 2022; Soltani et al., 2021a, 2021b), stainless steel die (Finnegan et al., 2022), KBr slide (González-Pleiter et al., 2021), and PTEF filter (Liao et al. 2021), each used in one study.

Detector The quality of the detector has a substantial impact on the speed of data acquisition and a high signal-to-noise ratio (more details in Text S1) (Cotruvo 2021). Studies using FTIR for MP detection mostly use a photoconductive (MCT) (Finnegan et al., 2022; González-Pleiter et al., 2021; Huang et al., 2021; Liu et al. 2019b, a; Wright et al. 2020) or pyroelectric detectors (DTGS) (Cai et al. 2017). In addition, for rapid chemical imaging, focal plane array (FPA) detectors have also been used in 2 studies (Kernchen et al. 2022; Vianello et al. 2019).

Background and baseline subtraction Background and baseline subtraction are the most commonly used forms of spectral processing methods that help to better analyze the peaks of interest (more details in

Table 8
Essential parameters in analysis M/NPs by FTIR (sorted by the type of substrate).

paper	Substrate	Detector	Spectral Range (cm^{-1})	Mode	Type of instrument	Number of Scans	Resolution	Spectral Processing	HQI (%)	Library
(Liu et al. 2019c)	glass fiber filter	MCT	4000–675	transmission	μFT-IR	16	4 cm − 1	background subtraction (CO2 and H2O)	60<	OMNIC spectra library
(Liu et al. 2022b)	glass fiber filter				μFT-IR				90<	Chemistry Database, Shanghai Institute of Organic Chemistry
(Szewc et al. 2021b)	glass fiber filter		4000–500	ATR	FT-IR	64	4 cm − 1			Hummel Polymer Sample Library, HR Nicolet Sample Library, Sigma Biological Sample Library, and Organics by Raman Sample Library
(Wang et al. 2020)	glass fiber filter			transmission	μFT-IR				70<	
(Ding et al. 2021b)	glass fiber filter				μFT-IR			background subtraction	70<	OMNIC polymer reference spectral library
(Liu et al. 2019a)	glass fiber filter	MCT	4000–675	transmission	μFT-IR	64	8 cm − 1	background subtraction (CO2 and H2O)	60<	OMNIC spectra library
(Cai et al. 2017)	glass fiber filter	DTGS	4000–500	reflection	μFT-IR					databases offered by Thermo Fisher Scientific inOMNIC software
(Amato-Lourenço et al. 2022)	glass (micro) fiber				FT-IR			baseline adjustment and removal of carbon dioxide (CO2)	60<	HR Hummel Polymer and Additives Aldrich condensed phase
(Liu et al. 2022b)	glass (micro) fiber		4000–500		μFT-IR				70<	
(Wright et al. 2020)	silver membrane filter	MCT	4000–500	reflection	μFT-IR	16	4 cm − 1	background subtraction	90<	Bio-Rad KnowItAll IR Spectral Library).
(Chen et al. 2022)	Silver filter				FT-IR				70<	Aldrich Polymers, Aldrich Polymers, Hummel Polymer and Additives, Rubber Compounding Materials, Polymer Additives and Plasticizers, Polymer Additives and Plasticizers, Sprouse Polymers by ATR, Sprouse Polymers by Transmission
(Dris et al. 2017)	quarts filter			ATR	μFT-IR					
(Huang et al., 2021)	nitrocellulose filter	MCT	4000–650	reflection	μFT-IR	64	8 cm − 1		60<	
(Liao et al. 2021)	PTEF filter		4000–675	transmission	μFT-IR	16	8 cm − 1		70<	OMNIC polymer spectra library
(Knobloch et al. 2021b)	calcium fluoride(CaF2) diamond compression window		4000–1000		μFT-IR		4 cm − 1		70<	Perkin Elmer FIBERS3, Perkin Elmer fiberfbi, Perkin Elmer fibers2, Perkin Elmer POLYADD1, Hummel Polymer Sample Library,

(*continued on next page*)

Table 8 (*continued*)

paper	Substrate	Detector	Spectral Range (cm^{-1})	Mode	Type of instrument	Number of Scans	Resolution	Spectral Processing	HQI (%)	Library
										Thermofisher Scientific Coatings Technology, Thermofisher Scientific Synthetic Fibers by Microscope, Georgia State Forensic Automobile Paints, Hummel Polymer and Additive, Sprouse Polymers by Transmission, Sprouse Polymers by ATR, Sprouse Polymer Additives, Thermofisher Scientific Industrial Coatings, Thermofisher Scientific Polymer Additives, and Plasticizers, Thermofisher Scientific Commercial Materials Polypropylene Additives, Thermofisher Scientific Commercial Materials Epoxy Compounds
(Kernchen et al. 2022)	calcium fluoride(CaF2)	FPA	1250–3600	transmission & ATR	μFT-IR	6	8 cm − 1			
(González-Pleiter et al. 2021b)	KBr slide	MCT detector	4000–550	transmission	μFT-IR	64	8 cm − 1		65<	built-in database or with a reference spectra specifically created for this study.
(Vianello et al. 2019)	ZnSe window	FPA	3750–850	transmission	μFT-IR	30	8 cm − 1	background subtraction		
(Soltani et al., 2021a, 2021b)	gold coated slide		4000–650	reflection	μFT-IR			background subtraction	70<	proprietary libraries in OMNIC Spectra software
(Finnegan et al., 2022)	stainless steel die gold mirror slide	MCT detector	4000–700	reflection	μFT-IR	64	4 cm − 1	background and baseline subtraction	80<	Perkin Elmer spectral libraries
(Zhang et al. 2020)	diamond compression window		4000–650	transmission	μFT-IR	16			70<	
(O'Brien et al. 2020)			4000–400	absorbance	FT-IR		16 cm − 1	background subtraction	80<	ATR Polymer Introductory Library, Perkin Elmer
(Dong et al. 2021)			4000–650	ATR	μFT-IR				70<	

FPA: focal plane array; MCT: mercury cadmium telluride; DTGS: deuterated triglycine sulfate; CaF_2: calcium fluoride; KBR: potassium bromide; PTEF: polytetrafluoroethylene; ZnSe: zinc selenide; CO_2: carbon dioxide; HQI: high quality index.

Text S1)(Cotruvo 2021). Based on this review, only 9 FTIR studies reported background subtraction in their methodology(Amato-Lourenço et al. 2022; Ding et al., 2021a; Finnegan et al., 2022; Liu et al. 2019b, a; O'Brien et al. 2020; Soltani et al., 2021a, 2021b; Vianello et al. 2019; Wright et al. 2020).

Hit Quality Index (HOI) library searching is used for microplastics identification, in which a characteristic vibrational spectrum (so-called fingerprint) is compared to a reference spectra library, and the similarity are estimated as Hit Quality Index (HQI) described in a normalized range between 0 % and 100% or between 0 and 1 (Rocha-Santos et al. 2022). The most used libraries in our review were the OMNIC polymer reference spectral library, Hummel Polymer Sample Library, and Perkin Elmer spectral libraries (Table 8). In this context, 9 studies recommend at least an HQI of 70% for MPs identification (Chen et al. 2022; Ding et al., 2021a; Dong et al. 2021; Knobloch et al. 2021a; Liao et al. 2021; Liu et al. 2022b; Soltani et al., 2021a, 2021b; Wang et al. 2020; Zhang et al. 2020) while 4 experiments suggested an HQI greater than 60% (Amato-Lourenço et al. 2022; Huang et al., 2021; Liu et al. 2019b, a).

Limit of Detection (LOD) In this review, we found that the smallest particle size that can be detected by FTIR is in the range of 10 μm to 20 μm(Lux et al. 2022; Rocha-Santos et al. 2022). However, in a study conducted by (Vianello et al. 2019) the lower limit of the applied FPA-FTIR was adjusted to 11 μm for the major dimension and 5.5 μm for the minor dimension.

3.4.7. Raman spectroscopy

Raman spectroscopy is a nondestructive method that uses a monochromatic light (laser beam) and provides information about the sample structure through a light scattering process. Plastics are usually quite Raman active and therefore show intense Raman spectra. Along with chemical identification, Raman can acquire information regarding morphology, particle size, and size distribution when the Raman spectrometer is coupled to a microscope called Raman spectromicroscopy or micro-Raman spectroscopy (Rocha-Santos et al. 2022; Vandenabeele 2013). In our review, 16 experiments utilized Raman analysis for chemical identification of airborne MPs, 15 of which used a micro-Raman spectrometer (Table 9).

substrate To achieve a high-quality and reliable Raman analysis, the selection of an appropriate substrate is essential (see Text S2). (Rahman et al. 2021; Rocha-Santos et al. 2022). According to our review, different types of filters or substrates were used for Raman analysis (Table 9) including S&S filter papers in 3 experiments, cellulose filters in 1 study, Aluminum oxide membrane filters in 2 studies, and glass (micro)fiber filters in 3 experiments. Moreover, other studies have used quartz, Teflon filters, silver membrane filters, polytetrafluoroethylene (PTEF), polycarbonate membranes, mixed cellulose ester membranes, two-sided copper adhesives, alumina-based membranes, and CaF_2 as the substrate for Raman analysis (Abbasi et al., 2022a; Nematollahi et al., 2022; Rahman et al., 2021; Trainic et al., 2020; Wright et al., 2019; Yao et al., 2022; Abbasi et al., 2022b). (Xu et al. 2020) utilized Klarite substrate, which is an exceptional SERS substrate and is shaped as a dense grid of gold inverted pyramidal cavities to detect atmospheric MPs smaller than 1 μm by Raman spectromicroscopy. It was illustrated that although Teflon filters, PTEF, aluminum-based filters, mixed cellulose ester, polycarbonate, and quartz filters are not suitable for Raman imaging, silver membrane filters have been considered suitable substrates for Raman analysis (more details in Text S2)(Rahman et al. 2021; Wright et al. 2019).

Laser power and wavelength An key parameter affecting the results obtained by Raman spectroscopy is the intensity of the laser and its wavelength (Text S2) (Wieboldt 2010). In order to reduce damage to the sample and filter, the laser power was controlled in some studies (Ferrero et al. 2022; Trainic et al. 2020; Welsh et al. 2022; Yao et al., 2022) (Table 9).

Grating, Acquisition time, and Number of scans Another way to improve the signal-to-noise ratio (≥3 acceptable) is to increase the number of lines of the grating (Text S2), measurement time and the number of scans (Rocha-Santos et al. 2022; Wieboldt 2010). Acquisition time is also known for its ability to affect spectral intensity and signal-to-noise ratio. (Rahman et al. 2021) described in detail that they increased the laser acquisition time from 2 s up to 10 s, in order to obtain spectra with a high signal-to-noise ratio for particles smaller than 500 nm. They also used 4 accumulations for obtaining the spectra of particles larger than 500 nm and 6 accumulations for particles smaller than 500 nm.

Background and baseline subtraction In order to have a better interpretation of Raman spectra, background and baseline subtraction is crucial (Text S2). The main source of baselines in Raman analysis is fluorescence, which can overwhelm Raman signals (Rocha-Santos et al. 2022). Of the papers reviewed, only one study presented that the aim of using a 532 nm laser was to reduce fluorescence(Ferrero et al. 2022). Some studies used confocal Raman microscopes containing an aperture objective lens and a confocal hole that suppresses fluorescence signals to remove fluorescence (Rahman et al. 2021; Xu et al. 2020; Yao et al., 2022).

HQI In this review, seven studies reported the HQI for library searching. In a study by (Kernchen et al. 2022) for spectral identification, an HQI of greater than 5 was accepted for MPs identification. (Rahman et al. 2021) identified particles as MP with HQI values of 0.70–0.98. Moreover, the main characteristic peak positions were used to identify microplastics in one experiment (Yao et al., 2022). Also, only one study used both HQI and matching peak wavenumber position to identify the composition of MPs (Wright et al. 2019).

LOD Raman spectroscopy can achieve a better spatial resolution (down to 1 μm) than FTIR (10 μm). (Rocha-Santos et al. 2022). In a study conducted by (Xu et al. 2020)., the synthesized single microplastic particles, with sizes down to 360 nm, and atmospheric microplastics with sizes down to 450 nm were detected and identified. Moreover, (Rahman et al. 2021) identified plastic particles with a nanometer range size (<1μm).

3.4.8. Scanning electron microscopy with energy dispersive X-ray (SEM-EDX)

SEM-EDX analysis provides a fast non-destructive elemental composition of the particles (mainly carbon and oxygen) by utilizing an electron beam. Therefore it is unable to characterize complex polymers (Abbasi et al. 2017; Abbasi et al., 2022c; Nematollahi et al. 2022; Yao et al., 2022). Based on the spectra, this method allows the detection of particle contamination, along with the determination of the degree of weathering and oxidation of MPs (Abbasi et al., 2022a; Yao et al., 2022; Abbasi et al., 2022b). Seven of the identified studies used SEM, all of which were coupled with EDX. They illustrated that airborne MPs mainly contain carbon and oxygen, which could bind a variety of trace elements to the surface (Abbasi et al., 2017, 2019, 2022a,c; Nematollahi et al., 2022; Yao et al., 2022; Abbasi et al., 2022b). Aluminum (Al), calcium (Ca), silicon (Si), titanium (Ti), and magnesium (Mg) are the most commonly described trace elements and sources of contamination. Yao and colleagues were the only ones to use the oxygen to carbon (O/C) ratio at the surface of particles as an indicator of weathering (Yao et al., 2022).

Coating As MPs are nonconductive samples, they must be coated with an electrically conductive surface such as gold to inhibit charging, reduces thermal damage, and enhances the secondary electron signal. (see section 4.1.)(Table 10).

3.4.9. Thermal degradation methods

Another method to analyze the chemical composition of MPs is thermal analysis such as pyrolysis gas chromatography-mass spectrometry (Pyr-GC/MS), thermogravimetric analysis gas chromatography-mass spectrometry (TGA-GC/MS), thermal extraction, and desorption gas chromatography-mass spectrometry (TED-GC/MS). These methods do not allow size determination of the particles but will determine the chemical composition and the concentrations of the individual chemical components. Based on this review, 3 studies used thermo analytical methods, (Peñalver et al. 2021) used thermogravimetric mass analysis and (Goßmann et al. 2022) and (O'Brien et al. 2020) used Pyr-GC/MS (see Text S3) for MPs chemical identification in their experiments which have been collected from the air, with a limit of detection of about 1 μg or sometimes lower.

Pyr-GC/MS In order to perform reproducible analysis with pyrolysis coupled to gas chromatography some parameters needs to be addressed.

Pyrolizer In order to analyze M/NPs through pyrolysis, the pyrolysis chamber needs to be rapidly heated and the temperature should be sufficiently transferred to the samples. This strongly depends on the type of pyrolizer (more details in supplementary). The two studies that applied Pyr-GC/MS, both used a micro-furnace pyrolizer (Goßmann et al. 2022; O'Brien et al. 2020).

Temperature and duration The temperature, the speed at which it is reached and the time at which it is maintained are key parameters in this method. The two studies reported temperatures of 650 °C (O'Brien et al. 2020) and 590 °C (Goßmann et al. 2022). However, there is currently no

Table 9
Essential parameters in analysis of M/NPs by Raman.

Reference	substrate	detector	mode	spectral range (cm^{-1})	laser wavelength (nm)	laser power (mW)	acquisition time (s)	number of scans	grating (lines/mm)	spectral processing	HQI (%)
(Klein and Fischer (2019))	slide	–	–		–	–	–	–	–	–	–
(Abbasi & Turner 2021a)	S&S filter	–	–	400–1800	785		–	–	–	–	–
(Wright et al. 2019)	•quartz microfiber •PTEF •mixed cellulose ester membrane •alumina-based membrane •silver membrane	CCD	imaging	centered at 1300	785	adjustable power (4–19)	2	–	600		HQI & matching peak wave number positions
(Ferrero et al. 2022)	Glass microscope slide	CCD	manual measurement	centering the spectral range on 1090	532	controlled laser power	a quick 1-second test, with 5 accumulations and the intensity of the laser fixed at 50%, was carried out at the border of each microparticle; if too intense, 60 accumulations of 1 s with a laser intensity of 5–10% were used	–		baseline subtraction	65<
(Kernchen et al. 2022)	Aluminum oxide	CCD	automatic particle detection	150–3600	532	5	0.5	5	600	using 532 nm laser to reduce fluorescence	> 5
(Welsh et al. 2022)	glass fiber	–	–	0–1800	532 and 785	adjustable power (0–85)	–	–	–	–	–
(Abbasi et al., 2022c)	S&S filter papers	–	–	400–1800	785		20 and 30	–	–	–	–
(Yao et al., 2022)	quartz	EMCCD	–		532	adjustable power (2.7–2.9)	–	–	600	a background subtraction using a rounded shape fit was applied to remove fluorescence	The main characteristic peaks
(Liu et al., 2022c)	glass fiber	–	–	0–4000	785 and 532	–	10–15	–	–	confocal Raman microscope –	> 70
(Xie et al. 2022)	alumina-based membrane	CCD	–	100–3500	532	15	10	–	–	background correction and cosmic ray removal	> 75
(Rahman et al. 2021)	CaF_2 slide Teflon filter Silver membrane filters	–	automatic particle detection	500–3400	532	10	2	6–10	1200	The FLAT correction was applied in order to remove background interference due to fluorescence.	0.70–0.98
(Abbasi et al. 2022b)	two-sided Cu adhesive tapes	–	–	400–1800	785	–	–	–	–	confocal Raman spectrometer –	–
(Xu et al. 2020)	Klarite	EMCCD	mapping	200 to 2000 cm − 1	785	25	5	15–50	1200	confocal Raman spectrometer	–

(*continued on next page*)

Table 9 (*continued*)

Reference	substrate	detector	mode	spectral range (cm^{-1})	laser wavelength (nm)	laser power (mW)	acquisition time (s)	number of scans	grating (lines/mm)	spectral processing	HQI (%)
										baseline removal was performed using LabSpec 6 software by a polynomial equation	
(Nematollahi et al. 2022)	two-sided Cu adhesive tapes	–	–	400–1800 cm − 1	785	–	–	–	–	–	–
(Abbasi et al., 2022a)	S&S filter papers	–	–	400–1800	786 nm	–	–	–	–	–	–
(Trainic et al. 2020)	Polycarbonate filter	CCD	automatic particle detection	100–3500	633 nm (but 532 and 785 nm were occasionally used as well)	–	–	–	600 g/mm	background subtraction	–

Cu: cupper; PTEF: polytetrafluoroethylene; HQI: high quality index; CaF2: calcium fluoride; CCD: charge-coupled devices; EMCCD: electron-multiplying charge-coupled device.

Table 10
Essential parameters in analysing airborne M/NPs by ESM-EDX.

Reference	coating	trace elements	Source of contaminants
(Abbasi et al., 2022c)	gold-coated	C, O, Al, Ca, Mg, Fe, Si, and Ti	geochemical sources
(Yao et al., 2022)	Ir-coated	C, O, Al, Ca, Mg, Fe, Si, Ti, P, Cl, Na, and S	different sources
(Abbasi et al. 2022b)	gold-coated	Al, Ca, Mg, Si, and Ti	–
(Abbasi et al. 2019)	–	C, O, Al, Ca, Si, Na, I and Mg	C, O, Al, Ca, Si, and Mg: contamination by extraneous solids such as dust and soil Na and I: material used for sample preparation
(Nematollahi et al. 2022)	gold-coated	C, O, N, Na, Mg, Al, Si, Cl, Ti, Mn, Cu, Zn, Sn, Sb, Hg, and Pb	Al, Si, Na, Mg, and Mn: silicate minerals (e.g., clays) Pb, Hg, Sb, Sn, Zn, Cu, and Ti: anthropogenic activities
(Abbasi et al. 2017)	–	C, O, Si, Ca, Mg, Al, S, Na, Fe, and K	Si-rich indicating geologic origin
(Abbasi et al., 2022c)	gold-coated	C, O, N, Zn, Cl	Zn, cl: contamination by residual ZnCls during the density separation process

consensus on the appropriate temperature to identify all polymers (Rocha-Santos et al. 2022). Only one study reported heating their samples for 12 s (O'Brien et al. 2020). Furthermore, the temperature gradient from the pyrolysis step to other next steps (GC and MS) is a crucial parameter that needs to be maintained at the highest temperatures to avoid high molecular weight molecules being created and trapped (Rocha-Santos et al. 2022). In a study conducted by O'Brien and colleagues, the pyrolyzer interface and GC injection port temperature were set at 300 °C and the GC oven temperature was held at 40 °C for 2 min, and then increased to 320 °C at 20 °C min^{-1}, then held for 14 min (O'Brien et al. 2020). However, Goßmann and colleagues did not provide this information (Goßmann et al. 2022).

Gas In a gas chromatographic method, the type of carrier gas and the flow rate are obviously important aspects (Rocha-Santos et al. 2022)., Helium was used as the carrier gas in both Pyr-GC/MS- based studies (Goßmann et al. 2022; O'Brien et al. 2020). One study made no mention of the flow rate (Goßmann et al. 2022), while the other used a constant linear flow of helium gas at 1.0 mL/min (O'Brien et al. 2020).

TGA-MS A TGA measures the change in weight of a sample as a function of temperature. According to our review, Peñalver et al. identified MPs by analyzing degradation products eluding from their MPs sample. The components in a gaseous phase were then injected into a quadrupole MS without chromatographic separation (Peñalver et al. 2021). This method also has specific parameters that should be taken into account.

Heating rate However, the same TGA results were shown for all MP sizes with increasing heating rate (Tondl et al. 2018), (Peñalver et al. 2021)gradually heated their samples from 30 to 800 °C at the rate of 10 °C/min.

3.4.10. Quantification

Besides characterization, quantification of airborne M/NPs is another crucial step to estimate exposure. Atmospheric M/NPs can be quantified in several ways, depending on the type of sampling and the matrix from which the M/NPs are separated. Overall, for active sampling with a pump, quantification is expressed as the number of M/NPs per volume of air (n/m^3), while for passive sampling it is expressed as the number of M/NPs per area (n/m^2) or weight (ng/m^2) of dust from which M/NPs were separated. In addition, the quantification of the M/

NPs collected through passive methods can also be expressed as deposition rate (n/m^2/day) (Rocha-Santos et al. 2022). According to our review, we identified 37 experiments reporting quantitative MP data (Table S5). Almost all active sampling strategies quantified particles as n/m^3, and only one experiment quantified MPs as ng/m^3 because of using TGA-MS in analytical technique (Kernchen et al. 2022). In the studies that used a passive sampling strategy, 9 studies quantified airborne M/NPs as a deposition rate (Huang et al., 2021; Klein and Fischer, 2019; Knobloch et al. 2021a; Liu et al. 2022b; Soltani et al., 2021a, 2021b; Szewc et al. 2021a; Welsh et al. 2022; Wright et al. 2020; Zhang et al. 2020), while 6 studies described them as the number of particles per gram sample, 4 of which were conducted in dust settled matrix (Abbasi et al. 2017; Abbasi & Turner 2021a; Abbasi et al., 2022c; Goßmann et al. 2022; Liu et al. 2022b; Nematollahi et al. 2022). Furthermore, 2 studies used a passive sampling strategy to quantify the MPS as a number of particles per volume, because they aimed at identifying MPs in water (Abbasi et al. 2022b; Dong et al. 2021). Among the studies reviewed, there is no unified statistical method for reporting M/NP pollution. Although some studies report did not provide the concentration of airborne M/NPs some describe it by a range, some used an average and some used both(Table S5).

Along with the field samples, the blank samples need to be quantified in order to show the extent of contamination in the field samples. According to this review, 32 out of 41 studies used blanks at different steps. Nonetheless, only 20 studies reported on the quantification of these blank samples. No contamination was reported in the blank samples in 8 studies (Supplementary table 5) (Abbasi et al., 2019, 2022a,c; Ding et al., 2021; Goßmann et al., 2022; Liu et al., 2019; Welsh et al., 2022; Xie et al., 2022; Abbasi et al., 2022b), while small numbers of M/NPs or MRs were reported in 12 other experiments (Abbasi et al. 2017; Amato-Lourenço et al. 2022; Chen et al. 2022; Kernchen et al. 2022; Klein and Fischer, 2019; Liao et al. 2021; Liu et al. 2022b; Liu et al. 2022b; O'Brien et al. 2020; Vianello et al. 2019; Wright et al. 2020; Zhang et al. 2020). These background values were then used to correct the data from the actual research samples. In an experiment conducted by (Kernchen et al. 2022), 28 blanks were utilized 9 of which were reported as having no contamination, while the rest of the blank samples contained variable amounts of MP. In another study, background contamination was considered negligible compared to field samples (Liao et al. 2021).

3.5. Contamination avoidance

To obtain reliable data on airborne MPs, it is essential to limit sample contamination at all stages of the study (Prata et al. 2021).

3.5.1. Pre-sampling

Filter pretreatment is one of the major steps for contamination avoidance before collecting samples, which in turn leads to quality assurance of the experiment. According to the articles reviewed (Table 1), filters were pretreated in 16 experiments, 13 of which used high temperatures for a specified time, one study utilized a microscope to examine the filters, and the other experiment flushed filters with nitrogen. Moreover, in a study conducted by (Amato-Lourenço et al. 2022), filters were weighed before collecting particles.

While filter pretreatment is one of the fundamental measures to achieve this goal in the pre-sampling step, some other serious measures are needed such as prefiltering reagents and solutions, cleaning or rinsing the equipment with various kinds of solutions (Milli Q water, deionized water, Ethanol, phosphate-free-soap, etc.). Contamination can be prevented by storing pre-cleaned filters, glassware, and other equipment in pre-baked Aluminum foils, and limiting plastics use by removing plastic components as described in some of the studies (Abbasi & Turner 2021a; Liu et al. 2019b; O'Brien et al. 2020). According to our review, most papers utilize one or more methods to reduce contamination (Table 1), while only an experiment conducted by Wright et al., 2020 specifies which step (pre-sampling) measures were taken. They washed all glassware with filtered ethanol and filtered ultra-pure water once and 3 times respectively to remove all plastic components prior to use. Along with this, Trainic et al., 2020 collected samples from all the devices in the sampling area In order to assure that the collected microplastics they identified were not emitted from any surface of the location.

3.5.2. Sampling

During sampling, microplastics not originally found in the environment can enter the sample, known as procedural contamination (Gwinnett & Miller 2021). Generally, different methods and measures are used to reduce procedural contamination; including 1/ wearing non-synthetic polymer clothing, e.g., cotton lab coats and nitrile gloves, 2/ delaying sample collection s to prevent contamination by the experimenter, 3/ processing samples within laminar flow hoods, or 4/ controlling laboratory air secluded rooms with controlled airflow (Abbasi et al., 2022a; Dong et al., 2021; Knobloch et al., 2021a; O'Brien et al., 2020; Rahman et al., 2021; Amato-Lourenço et al., 2022). Moreover, placement of the sampler in a position that avoids resuspension of ground dust or that is far away from other factors that cause pollution (Chimney in cruise sampling) is an important consideration when collecting samples (Ding et al., 2021a; Liu et al. 2019b; Wang et al. 2020). Another effort to eliminate contamination during sampling is to stand downwind during sampling and keep an appropriate distance from the sampler (Liu et al. 2019a; Wright et al. 2020). In addition, some studies take blanks or control samples alongside their environmental samples to ascertain the level of contamination. Of the studies reviewed, 23 used blanks to assess background contamination during the sampling procedure. Based on this review, almost all papers used measures to eliminate contamination during the experiment but did not specify them as procedural contamination measures, except in one study performed by Wright et al.(Wright et al. 2020).

3.5.3. Post-sampling

Strict measures are needed to prevent plastic and fiber contamination during the treatment and preparation steps (post-sampling) (Liu et al. 2019b). Although the majority of the articles reviewed did not exactly specify the contamination avoidance procedure for the preparation step, they unified on some points for this goal. Wearing a cotton lab coat(Abbasi et al., 2022a; Dong et al., 2021; Goßmann et al., 2022; Huang et al., 2021; Knobloch et al., 2021a; Rahman et al., 2021; Welsh et al., 2022; Xu et al., 2020; Abbasi et al., 2022b), covering all opening parts with Aluminum foil(O'Brien et al. 2020), covering filters with Aluminum foil or glass lid while drying(Dong et al. 2021; Goßmann et al. 2022; Knobloch et al. 2021a; Xie et al. 2022; Xu et al. 2020), working under laminar flow (Dong et al. 2021; Liao et al. 2021; Rahman et al. 2021; Wright et al. 2020), and using a cleaned laboratory bench(Abbasi et al., 2019, 2022a,c; Liu et al., 2022b; Nematollahi et al., 2022; Abbasi et al., 2022b) are the main measures taken to reduce contamination from the post-sampling step. Additionally, in 13 articles, blank samples were utilized during the treatment and preparation step to increase the accuracy of the experiment because this can illustrate the number of plastic and fiber contaminants along with the procedure (Abbasi et al., 2019, 2022a; Dong et al., 2021; Ferrero et al., 2022; Huang et al., 2021; Kernchen et al., 2022; Klein and Fischer, 2019; Liao et al., 2021; Liu et al., 2022b; Vianello et al., 2019; Welsh et al., 2022; Xu et al., 2020; Yao et al., 2022; Abbasi et al., 2022b). Avoiding the use of plastic and utilizing glassware or metalware in this step is another approach used in 3 experiments (Knobloch et al. 2021a; Rahman et al. 2021; Xu et al. 2020). Three studies used glass pipettes to transfer their samples to the substrate instead of plastic(Knobloch et al. 2021b; Rahman et al. 2021; Xu et al. 2020).

3.5.4. Analysis and quantification

To obtain reliable results and conduct a well-qualified study, it is essential to limit sample contamination at all stages of the study, from

sample collection to analysis in the lab. Although the majority of reviewed studies did not specify the protocols to avoid contamination during the analysis step, 34 studies explained some measures taken during sample screening. Common laboratory practices include wearing a 100% cotton lab coat and disposable nitrile gloves, performing analyses in an ultra-clean stainless steel room, cleaning all surfaces with ethanol, and using blank samples. For instance, (Nematollahi et al. 2022) described that the laboratory equipment and benches were cleaned with ethanol and paper wipes before performing sample analysis. Wright et al. covered the microscope with a plastic curtain to minimize deposition(Wright et al. 2020). Moreover, Rahman and colleagues covered the samples with a CaF_2 coverslip while using objective X100 before visualizing them(Rahman et al. 2021). In another experiment conducted by O'Brien et al., in order to analyze samples with pyrolysis-GC/MS, a new sample cup for each sample was used(O'Brien et al. 2020). One study also described that the humidity of the laboratory was increased through a pressure sprayer and an air filter, resulting in less contamination (Klein and Fischer, 2019). To avoid contamination during the quantification and identification step, image acquisition was directly performed on the 25-μm stainless steel filters placed into their closed Petri dishes (González-Pleiter et al., 2021).

4. Discussion

Plastics are ubiquitous and pervasively present in every part of the environment (Eriksen et al. 2013; Ferrero et al. 2022; Scheurer & Bigalke 2018). Atmospheric micro- and nanoplastics have been a growing concern in recent decades (Ferrero et al. 2022; Klein and Fischer, 2019; Liao et al. 2021). These airborne particles are transported by the wind, deposited, resuspended, cross boundaries, and in this way, they can affect human health after inhalation and/or ingestion (Abbasi et al. 2019; Liu et al. 2019a; Nematollahi et al. 2022; Soltani et al., 2021a, 2021b; Vianello et al. 2019). At present, methodological and technical limitations, as well as differences in data analysis and reporting, make an accurate estimation of airborne M/NPs prevalence difficult. This is a review of airborne M/NPs studies that critically discusses the main issues associated with the analysis of M/NPs in the atmosphere. The included studies (n = 41) used different sampling and characterization methods (Table 11). Often the methodologies presented are incomplete, thereby hampering the reproducibility and understanding of the techniques.

4.1. Collecting required information

4.1.1. Matrix, sampling location, and settings

The first issues that need to be considered in MPs and NPs studies are the type of environment and matrix from which samples will be collected. This will determine the methodological approaches for collecting particles and sample treatment for further analysis. According to the aim of the study, the sampling location, for both indoor or outdoor settings, needs to be carefully defined in terms of distance to the source of M/NPs (highways, manufactures, …), population density (urbanized/non-urbanized), traffic density, and also other spatial characteristics such as land use and vegetation (Klein and Fischer, 2019).

4.1.2. Meteorological factors

Weather conditions are known to easily influence the distribution, abundance, and source of atmospheric MP and NPs. Therefore, recording and pointing out these conditions during sampling should be present in all studies. (Liu et al. 2019b).

4.1.3. Height of sampling

Based on the research question and the aim of the study, the sampling height needs to be well chosen,(Rocha-Santos et al. 2022). To have a representative sample of the atmospheric environment while avoiding interference from human activities, atmospheric fallout or suspended

Table 11
Overview of pros and cons of different methods in sampling and analytical techniques of airborne m/nps.

Technique	Advantage	Disadvantage
Sampling		
Passive	Easy to apply	Increase contamination from the environment
	Helpful for meteorological factors influences	Underestimation of small particles
Active	Reproducible	Energy input requirement
	Sample suspended smaller particles	
Visual Analysis		
Stereomicroscope	Non– destructive	Potential misidentification
	Easy to use No sample preparationInformation on the physical characteristic of particles (number, size, shape, color)	No information on the particles' chemical compositionHigh limit of detection (50 μm)
Fluorescence microscopy		Partially destructive
	Reliable on the identification of plastic particle Identification of small MPsInformation on the physical characteristic of particles (number, size, shape)	Extensive sample preparation No information on the chemical composition of particles No information on the particles' color Similar material interferences; leading to an overestimation Possible contaminationIntermediate limit of detection (<50 μm)
Polarized light microscopy	Identification of small MPs Information on the physical characteristic of particles (size, shape)	Extensive sample preparation No information on the chemical composition of particles No information on the particles' color Similar material interferences; leading to an overestimation
SEM	Non– destructive Information on the physical characteristic of particles (number, size, shape, surface morphology)	Extensive sample preparation No information on the chemical composition of particles No information on the particles' color Possible contaminationLow limit of detection (nanometer size range)
Chemical Analysis		
FTIR	Non-destructive Low or no sample preparationPhysical characteristics of particles (number, size, shape, color) Information on the chemical composition of particlesLow limit of detection (>10 μm)	Long measurement time Possible destructing particles (depends on the mode)
Raman	Non-destructive Low or no sample preparationPhysical characteristics of particles (number, size, shape, color) Information on the chemical composition of particlesLow limit of	Long measurement time Possible burning of particles

(continued on next page)

Table 11 (*continued*)

Technique	Advantage	Disadvantage
	detection (>1 μm)	
PYR-GC–MS	No sample preparation Information on the chemical composition of particles Information on the additives correlated to particles Information on particle mass Less measurement time	Destructive No information on the Physical characteristic of particles (number, size, shape, color) Suitable for a small amount of samples
SEM-EDX	Non– destructive Information on the physical characteristic of particles (number, size, shape, surface morphology) Information on weathering degree of particles Information on contaminants related to particles	Extensive sample preparation No information on the chemical composition of particles No information on the particles' color Possible contamination
TGA-MS	No sample preparation Information on the chemical composition of particles Information on the additives correlated to particles Information on particle mass Suitable for a higher amount of samples Less measurement time	Destructive No information on the Physical characteristic of particles (number, size, shape, color) Information on the thermal behavior of samples Hardly coupled with GC leading to less accuracy

dust is collected at a different altitude above ground level (Liu et al. 2019b; Rocha-Santos et al. 2022). Yet, if a study aims to estimate human risk, it is essential to use the respiratory height (sitting 110 cm or standing 170 cm) (Amato-Lourenço et al. 2022; Chen et al. 2022; Vianello et al. 2019).

4.2. Sample collection

4.2.1. Choice of substrate

The choice of the substrate (composition, surface texture) and pore size are critical parameters (Rocha-Santos et al. 2022).

Composition: It is vital to consider a non-plastic made substrate or filter as it may interfere with chemical analysis (Amato-Lourenço et al. 2022; González-Pleiter et al., 2021; Liu et al. 2022b). In our review, 41% of papers used glass fiber filters for collecting and analyzing airborne plastic particles (Table 1).

Surface texture: In order to visualize particulates, the surface of the filters must be flat and nonstructured, as well as making particles immobile(Finnegan et al., 2022). Quartz(Wright et al. 2019) and Teflon (Rahman et al. 2021) filters were shown to have inappropriate features for good visibility of particulate matters, while they were used in 10% and 2% of studies, respectively.

Filter pore size: In terms of particle size, the filter pore size determines the lower size of particles that will be captured and hence the reported particle count. In our review, we showed that most experiments used filters with greater than 1 μm pore size, which facilitates the collection of larger MPs, avoids filter clogging but leads to an underestimation of the smaller particles (nanoparticles). (Rocha-Santos et al. 2022).

4.2.2. Sampling

There are two main methods to collect micro- and nano plastics in the atmosphere, passive and active sampling (Table 2) The differences between the two methods are mainly due to the fact that heavy, dense, and larger particles tend to settle, leading to over-representation when sampling surface deposits, while smaller particles can only be found through active sampling (Rahman et al. 2021).

Passive methods are in general easier to apply, requiring minimal and low-cost equipment including a brush or a funnel and an open container or artificial surface..

Active samplings involve the collection of suspended particles either by a pump or a cascade. One of the advantages of active sampling is the high level of reproducibility due to knowing the sampled air volumes. However, this type of method requires the implementation of standardized protocols, energy inputs, and specialized equipment.

In particular, these methods are complementary, so some studies aim to use both methods in order to have accurate results about atmospheric M/NP contamination (Rocha-Santos et al. 2022). In an experiment conducted during an oceanographic cruise, a combination of active and passive sampling characteristics, using a "deposition box", was utilized to overcome the limitation of using one sampling method. This system is designed to maintain a constant sampling of ambient air by a specific intake flow rate while maintaining a calm environment within.

4.3. Treatment and preparation

Obviously, not only plastic but also a lot more particles are in the air, such as organic and inorganic materials from the environment. So a focused treatment and preparation of the samples facilitates the quantification of specifically plastic particles more accurately (Stanton et al. 2019). The treatment procedures are chosen selectively based on the degree of contamination of the sample. Most studies (48%) performed oxidation steps to remove organic matter. Organic and mineral matter were more likely to be present in deposited dust samples than in suspended particle samples (Dehghani et al. 2017), so the treatment steps were mainly performed on samples collected from the non-air matrix (water and dust). Following the treatment step, a transfer of the sample from the filtration membrane to the analytical substrate is performed. Although such treatment may not change the size of larger MPs significantly, a small loss of surface material could have a significant impact on the submicron particles (Rahman et al. 2021; Vianello et al. 2019).

4.4. Analysis

4.4.1. Visual analysis

One of the most common and cheapest methods for MPs identification is visually examining particles under **light microscopy** (Rocha-Santos et al. 2022). Characterizing atmospheric MPs based on their morphology is a good way to guesstimate their sources (Cai et al. 2017). Although there are no standardized criteria for the visual identification of MPs, this method does not require complex extraction methods, and researchers can easily train themselves to identify MPs visually (Rocha-Santos et al. 2022). It is obvious that this technique and criteria are limited to large plastic particles, as the morphological features become less obvious with decreasing size, which in turn leads to an underestimation of smaller MPs (Wright et al. 2019).

. Concerning the notation of the color of particles, the light source (frequencies included) and the scattering of the light may lead to the misidentification of colors (Soltani et al., 2021a, 2021b). These shortcomings need to be considered using a light microscope.

The smaller plastic particles which are not distinguishable through light microscopy can be analyzed by **fluorescence microscopy** (Erni-Cassola et al. 2017). This method requires dye staining. The most commonly used fluorescent dye is Nile red, binding to the hydrophobic surface of plastics causes them to fluoresce, however, Nile red staining is not specific. In order to reduce the detection of false positives, an additional treatment, digestion, is essential to eliminate organic particles from the samples (Rocha-Santos et al. 2022). Another technique used in the analysis of M/NPs is **scanning electron microscopy (SEM)**,

which allows the investigation of the size and shape of particles down to a few hundred nanometers in size (Goldstein et al. 2018). MPs can also be identified through **polarized light microscopy** (size and shape) however some other materials like wood and paper polarized light microscopes exhibited similar behavior with MPs and can lead to misidentification (Abbasi et al. 2017).

4.4.2. Representative analysis

Visual inspection of airborne samples can only give a rough estimate of the N/MP in the sample examined. Therefore, microscopic analysis is usually performed first to identify particles that look like plastic particles. Second, a more specific spectroscopic assessment is performed on a smaller sub-sample of a specified mass to represent the entire sample (Rocha-Santos et al. 2022).

4.4.3. Size categorizing

Our review illustrates that the size classes of plastic particles vary widely between studies making the comparison of these data difficult. Therefore, we could not draw a clear conclusion regarding the size ranges between deposited and suspended particles from the available data. The reason for the lack of uniformity in the size classes is related to the pore size of the filter and the detection limits of the analytical techniques. Moreover, in order to be able to compare studies, the methods used to measure the particle size must also be specified. The most commonly used parameter for size detection in reviewed papers is the measure of longest length (Abbasi et al. 2019; Amato-Lourenço et al. 2022; Dris et al. 2017; Nematollahi et al. 2022; Szewc et al. 2021a; Wang et al. 2020).

4.4.4. Chemical analysis

Fourier-transformed infrared spectroscopy (FTIR) is the most popular chemical identification method (23 out of 39), followed by Raman (16 out of 39), while the thermal degradation methods are less used (3 out of 39).

As indicated earlier, **FTIR** and **Raman** are non-destructive techniques. Combining these methods with visual inspection improves the detection limit to 10 μm for FTIR and 1 μm for Raman which allows the detection of smaller particles (Rocha-Santos et al. 2022). However, plastics in the nanometer range can be detected by Raman spectroscopy by optimizing the method and instrument conditions such as the type of substrate for sample mounting. The main disadvantages of both methods (FTIR & Raman) are the time-consuming scanning procedure, the use of a specific type of filter, the requirement for the absence of contamination in the samples, expensive equipment, and the need for a well-trained operator, which makes it difficult to implement as routine analysis. Chemical identification of particles with FTIR or Raman can be performed by imaging or mapping techniques. One of the drawbacks of this method is the acquisition of a large number of spectra that subsequently needs to be compared to spectra in a library, which requires time and very good computational power; the library matching is based on calculating the correlation between unknown and known spectra from a library resulting in a Hit Quality Index (HQI) (Rocha-Santos et al. 2022).

Based on our review, two thermal degradation principles have been applied for the identification of airborne M/NPs, including **Pyr-GC–MS, TGA-MS,** and **TGA-GC/MS**, which are suitable for capable of the simultaneous characterization of polymer types, volatiles, and additives (Herrera et al. 2003). These are destructive methods and cannot determine the physical properties of the particles (shape, size, etc.) (Peñalver et al. 2021). Pyr-GC–MS is preferred for heterogeneous samples and can be applied for small sample weights (a few micrograms) (Dümichen et al. 2017; Wampler 2006), but has the limitation that pyrolysis of high molecular weight components of products can result in column clogging (Dümichen et al. 2017). TGA has emerged as an alternative, less expensive, faster, and easier technique that also can be coupled with MS leading to yield information about sample mass changes and chemical composition of degradation product at the same run (Duemichen et al. 2014; Gomes et al. 2018; Peñalver et al. 2021). (Duemichen et al. 2014; Gomes et al. 2018; Peñalver et al. 2021). One of the advantages of this technique is the use of a larger amount of sample for analysis (about 200 times larger than with Pyr-GC–MS) (Peñalver et al. 2021). Coupling TGA to a GC for separation prior to MS detection (TGA-GC/MS), is difficult and expensive to perform (Duemichen et al. 2014; Peñalver et al. 2021) and short-lived decomposition products cannot be detected with this method (Duemichen et al. 2014, 2015). This limitation can be surmounted by trapping the volatile products released from the polymer on a connected solid-phase adsorbent material (twister), followed by the analysis of the adsorbents on the twister by thermal desorption gas chromatography-mass spectrometry (TDS–GC–MS)(Duemichen et al. 2014). This process offers some advantages as there is no contamination of a transfer capillary occurs and the maintenance effort is very low (Dümichen et al. 2017). However, based on our review, the latter method has not been performed yet in atmospheric M/NPs samples.

4.4.5. Visual and chemical analysis

Coupling of **SEM with an energy dispersive X-ray spectrometer (EDS)** provides information on size, shape, and particle surface topography which in turn renders information regarding the aging or weathering of plastic particles together with elemental composition (Goldstein et al. 2018). One of the drawbacks of this method along with the high-priced equipment is the need for sample preparation, while the use of EDS leads to the possibility of particle loss during the mounting or coating step (Goldstein et al. 2018).

4.4.6. Quantification

Currently, there is no universally accepted method for the quantification of plastics, for this purpose. In the reviewed atmospheric micro- and nano plastic-studies there are large differences in the quantification methods, which depend on the type of sampling (Rocha-Santos et al. 2022). Overall, we have shown that the quantification of MPs or NPs are mostly reported as n/m^2/day in passive sampling studies, while it is generally described as n/m3 in active sampling experiments. Counting particles within the entire sample is not feasible because it is complex and prone to human error, especially for small particles within a sample with a high particle load(Rocha-Santos et al. 2022). Thus, in several studies, only a part of the samples was quantified and the total MP number was then extrapolated to the entire sample. For instance, in a study by (O'Brien et al. 2020)filters were divided into quarters and after being tested for homogeneity, particles were counted on a quarter with the least variability. In another study, two slices out of 8 equal slices of filters were randomly picked for observation (Zhang et al. 2020). It is noteworthy that a non-homogeneously distribution of particles can lead to over- and underestimation results. However, some studies used some methods to ensure that all areas of the filter were covered (Ding et al., 2021a Wang et al. 2020).

4.5. Contamination prevention

With an increase in M/NPs studies the knowledge of contamination avoidance during the experiment has also improved substantially. It is obvious that some precautions need to be taken to limit the contamination of samples and thus overestimation of the M/NPs concentration at all stages of the study, including pre-sampling, sampling, post-sampling, and analysis (Gwinnett & Miller 2021). However, as of yet, methods to prevent procedural contamination have not been standardized. Based on our review, 5 experiments reported no protocols to prevent contamination from entering the sample(Dris et al. 2017; Finnegan et al., 2022; Huang et al., 2021; Peñalver et al. 2021; Wright et al. 2019).

5. Future consideration on good practice measures

Based on our review, a good practice for M/NPs analysis should consist of the following steps (flow chart, Fig. 3).

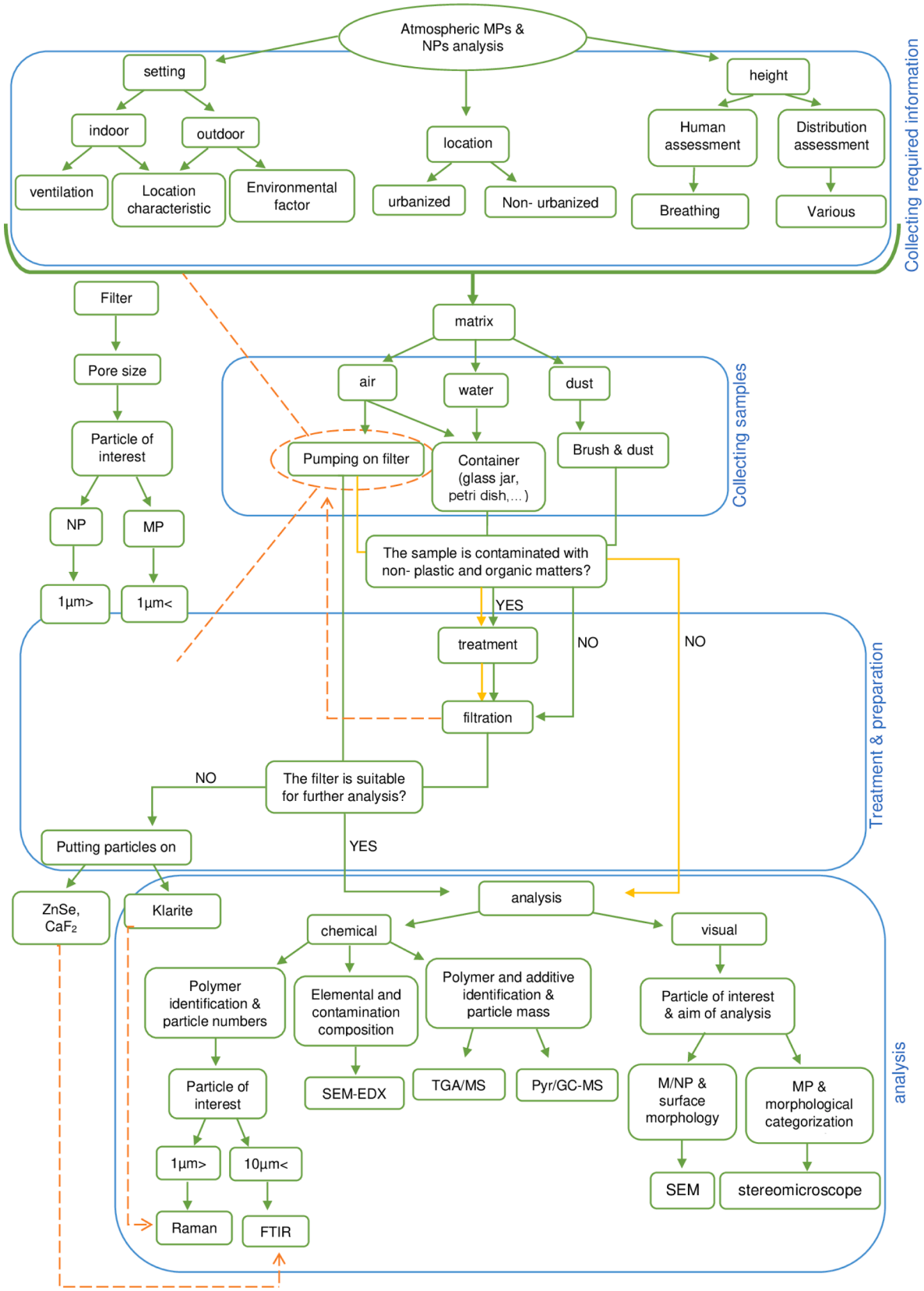

Fig. 3. Proposed flow chart for airborne M/NPs analysis. Explained in detail in the text. Yellow lines indicate the active sampling method. MP: microplastic; NP: nano plastic; PYR/GC–MS: pyrolysis/gas chromatography and mass spectroscopy; TGA/GC–MS: thermogravimetric analysis/ gas chromatography and mass spectroscopy; SEM: scanning electron microscopy. (For interpretation of the references to color in this figure legend, the reader is referred to the web version of this article.)

1. Sampling location and conditions

Depending on the research question, the sampling location needs to be carefully defined:

- Urbanization/rural status, distance to the source of M/NPs (e.g. highways, roads, industries, city center)
- indoor and/or outdoor setting
  - o architectural characteristics for indoor settings (area, height of ceiling, number of rooms, number of doors/ windows and their opening and closing status, floor covering) as well as the number of habitants and their age, the lifestyle of habitants (e.g. laundry, cleaning habits), ventilation and air conditioning status, temperature and, humidity
  - o for outdoor settings (pressure, humidity, temp, wind velocity, traffic density, population density, vegetation status)
- Breathing zone height for human exposure assessment and different heights for distribution study.

2. Sample collection

Based on the particle of interest (suspended/deposited and its size), the following needs to be addressed:

- Type of sampling (active/ passive)
- Filter pore size, the volume of filtered air (for active sampling), and composition of the filter (according to the analytical method used)

3. Analysis

To obtain comprehensive results, two major analyses are required:

- Visual (SEM and stereomicroscope) for shape, size, color, and surface morphology
- Chemical (FTIR, Raman, and Pyr/GC–MS) for polymer, additive, weathering, and contamination identification

4. Contamination prevention

To reduce the external contamination, blank samples and restrict measures are required in each step:

- Pre-sampling: burning filters at high temperature, cleaning sampling equipment with ethanol and/ or ultra-pure water, storing filters and equipment in pre-baked aluminum Aluminum foil after treatment, and replacing plastic components with suitable ones.
- Sampling: wearing non-synthetic polymer clothes and nitrile gloves, standing downwind, placing the sampler in an appropriate position (far away from the chimney, good height for resuspension avoidance), including a time delay between setting up the sampler and starting the sampling.
- Storage and transport: covering the filters and/or containers with Aluminum foil, transporting them immediately to the laboratory, and storing them at a specific temperature in the laboratory.
- Post-sampling (treatment and preparation): wearing non-synthetic polymer clothes and nitrile gloves, covering filters with Aluminum foil or glass lid while drying, working under laminar flow, and cleaning the laboratory bench with ethanol and/or ultra-pure water.
- Analysis: wearing non-synthetic polymer clothes and nitrile gloves, working in an ultra-clean stainless steel room, and cleaning all surfaces and equipment with ethanol and/or ultra-pure water.

6. Conclusion

This review clearly shows that different methods are used for sampling, preparation, and analysis of atmospheric micro- and nano plastics from different matrices such as water, dust, and air. Additionally, the review of the literature reveals that although Standard Operating Procedures (SOP) or standardized methods are required, the reporting of different units and sizes, the categorization of synthetic polymers based on their forms, shapes, and different sampling methods and analytical tools often hinder the comparability of results. According to our review, in order to have precise results regarding airborne M/NPs it is recommended to use several methods in both sampling and analytical steps. To our point of view, both passive and active methods are vital to acquire comprehensive samples of both settled and suspended M/NPs. In terms of analytical techniques, applying Raman and Pyr-GC/MS provide physicochemical characteristics together with additives related to particles. In addition, silver membrane filters are a suitable substrate with good visibility of particles on it and the least interference with chemical identification in Raman analysis. It is noteworthy that in order to have a reliable result it is encouraged to use the clean room or blank samples at each single step from sampling to analysis.

Funding

This work was supported by KU Leuven C3 Industrieel Onderzoeksfonds (3M200802).

Declaration of Competing Interest

The authors declare that they have no known competing financial interests or personal relationships that could have appeared to influence the work reported in this paper.

Data availability

Data will be made available on request.

Appendix A. Supplementary data

Supplementary data to this article can be found online at https://doi.org/10.1016/j.envint.2023.107885.

References

Abbasi, S., Alirezazadeh, M., Razeghi, N., Rezaei, M., Pourmahmood, H., et al. 2022b. Microplastics captured by snowfall: A study in Northern Iran. Sci. Total Env. 822.
Abbasi, S., Keshavarzi, B., Moore, F., Delshab, H., Soltani, N., Sorooshian, A., 2017. Investigation of microrubbers, microplastics and heavy metals in street dust: a study in Bushehr city, Iran. Environ. Earth Sci. 76 (23), 798.
Abbasi, S., Keshavarzi, B., Moore, F., Turner, A., Kelly, F.J., et al., 2019. Distribution and potential health impacts of microplastics and microrubbers in air and street dusts from Asaluyeh County, Iran. Environ. Pollut. 244, 153–164.
Abbasi, S., Rezaei, M., Ahmadi, F., Turner, A., 2022a. Atmospheric transport of microplastics during a dust storm. Chemosphere. 292, 133456.
Abbasi, S., Turner, A., 2021a. Dry and wet deposition of microplastics in a semi-arid region (Shiraz, Iran). Sci. Total Environ. 786, 147358.
Abbasi, S., Turner, A., 2021b. Dry and wet deposition of microplastics in a semi-arid region (Shiraz, Iran). Sci. Total Env. 786.
Abbasi, S., Turner, A., Sharifi, R., MohammadJ, N., Keshavarzifard, M., Moghtaderi, T., 2022c. Microplastics in the school classrooms of Shiraz Iran. Build. Environ. 207, 108562.
Amato-Lourenço, L.F., de Souza Xavier Costa, N., Dantas, K.C., dos Santos Galvão, L., Moralles, F.N., et al., 2022. Airborne microplastics and SARS-CoV-2 in total suspended particles in the area surrounding the largest medical centre in Latin America. Env. Pollut. 292.
Bhargava, R., Wang, S.-Q., Koenig, J.L., 2003. FTIR Microspectroscopy of Polymeric Systems. In Liquid Chromatography / FTIR Microspectroscopy / Microwave Assisted Synthesis, Vol. 163, pp. 137–91. Berlin, Heidelberg: Springer Berlin Heidelberg.
Cai, L., Wang, J., Peng, J., Tan, Z., Zhan, Z., et al., 2017. Characteristic of microplastics in the atmospheric fallout from Dongguan city, China: preliminary research and first evidence. Environ. Sci. Pollut. Res. 24 (32), 24928–24935.
Chen, E.-Y., Lin, K.-T., Jung, C.-C., Chang, C.-L., Chen, C.-Y., 2022. Characteristics and influencing factors of airborne microplastics in nail salons. Sci. Total Environ. 806, 151472.
Claessens, M., Meester, S.D., Landuyt, L.V., Clerck, K.D., Janssen, C.R., 2011. Occurrence and distribution of microplastics in marine sediments along the Belgian coast. Mar. Pollut. Bull. 62 (10), 2199–2204.
Cotruvo, J.A., 2021. Rare-Earth Element Biochemistry: Characterization and Applications of Lanthanide-Binding Biomolecules. Academic Press.
Dehghani, S., Moore, F., Akhbarizadeh, R., 2017. Microplastic pollution in deposited urban dust, Tehran metropolis, Iran. Environ. Sci. Pollut. Res. 24 (25), 20360–20371.

Ding, Y., Zou, X., Wang, C., Feng, Z., Wang, Y., et al., 2021b. The abundance and characteristics of atmospheric microplastic deposition in the northwestern South China Sea in the fall. Atmos Env. 253.
Ding, Y., Zou, X., Wang, C., Feng, Z., Wang, Y., et al., 2021. The abundance and characteristics of atmospheric microplastic deposition in the northwestern South China Sea in the fall. Atmos. Environ. 253, 118389.
Dong, H., Wang, L., Wang, X., Xu, L., Chen, M., et al., 2021. Microplastics in a Remote Lake Basin of the Tibetan Plateau: Impacts of Atmospheric Transport and Glacial Melting. Env. Sci Technol. 55 (19), 12951–12960.
Dris, R., Gasperi, J., Mirande, C., Mandin, C., Guerrouache, M., et al., 2017. A first overview of textile fibers, including microplastics, in indoor and outdoor environments. Environ. Pollut. 221, 453–548.
Duemichen, E., Braun, U., Senz, R., Fabian, G., Sturm, H., 2014. Assessment of a new method for the analysis of decomposition gases of polymers by a combining thermogravimetric solid-phase extraction and thermal desorption gas chromatography mass spectrometry. J. Chromatogr. A. 1354, 117–128.
Duemichen, E., Braun, U., Kraemer, R., Deglmann, P., Senz, R., 2015. Thermal extraction combined with thermal desorption: A powerful tool to investigate the thermo-oxidative degradation of polyamide 66 materials. J. Anal. Appl. Pyrolysis. 115, 288–298.
Dümichen, E., Eisentraut, P., Bannick, C.G., Barthel, A.-K., Senz, R., Braun, U., 2017. Fast identification of microplastics in complex environmental samples by a thermal degradation method. Chemosphere. 174, 572–584.
Eriksen, M., Mason, S., Wilson, S., Box, C., Zellers, A., et al., 2013. Microplastic pollution in the surface waters of the Laurentian Great Lakes. Mar. Pollut. Bull. 77 (1–2), 177–182.
Erni-Cassola, G., Gibson, M.I., Thompson, R.C., Christie-Oleza, J.A., 2017. Lost, but Found with Nile Red: A Novel Method for Detecting and Quantifying Small Microplastics (1 mm to 20 μm) in Environmental Samples. Environ. Sci. Technol. 51 (23), 13641–21368.
Ferrero, L., Scibetta, L., Markuszewski, P., Mazurkiewicz, M., Drozdowska, V., et al., 2022. Airborne and marine microplastics from an oceanographic survey at the Baltic Sea: An emerging role of air-sea interaction? Sci. Total Env. 824.
Finnegan, A., Süsserott, R.C., Koh, L.H., Teo, W.B., Gouramanis, C., 2022. A Simple Sample Preparation Method to Significantly Improve Fourier Transform Infrared (FT-IR) Spectra of Microplastics. Appl. Spectrosc. 37028221075065.
Free, C.M., Jensen, O.P., Mason, S.A., Eriksen, M., Williamson, N.J., Boldgiv, B., 2014. High-levels of microplastic pollution in a large, remote, mountain lake. Mar. Pollut. Bull. 85 (1), 156–163.
GENERAL AIR SAMPLING GUIDELINES. 1994.
Gigault, J., ter Halle, A., Baudrimont, M., Pascal, P.-Y., Gauffre, F., et al., 2018. Current opinion: What is a nanoplastic? Environ. Pollut. 235, 1030–1104.
Goldstein, J.I., Newbury, D.E., Michael, J.R., Ritchie, N.W.M., Scott, J.H.J., Joy, D.C., 2018. Scanning Electron Microscope (SEM) Instrumentation. In Scanning Electron Microscopy and X-Ray Microanalysis, pp. 65–91. New York, NY: Springer New York.
Gomes, J., Batra, J., Chopda, V.R., Kathiresan, P., Rathore, A.S., 2018. Monitoring and Control of Bioethanol Production From Lignocellulosic Biomass. In: Waste Biorefinery. Elsevier, pp. 727–749.
González-Pleiter, M., Edo, C., Aguilera, Á., Viúdez-Moreiras, D., Pulido-Reyes, G., et al., 2021. Occurrence and transport of microplastics sampled within and above the planetary boundary layer. Sci. Total Environ. 761, 143213.
González-Pleiter, M., Edo, C., Aguilera, Á., Viúdez-Moreiras, D., Pulido-Reyes, G., et al., 2021b. Occurrence and transport of microplastics sampled within and above the planetary boundary layer. Sci. Total Env. 761.
Goßmann, I., Süßmuth, R., Scholz-Böttcher, B.M., 2022. Plastic in the air?! - Spider webs as spatial and temporal mirror for microplastics including tire wear particles in urban air. Sci. Total Env. 832.
Gwinnett, C., Miller, R.Z., 2021. Are we contaminating our samples? A preliminary study to investigate procedural contamination during field sampling and processing for microplastic and anthropogenic microparticles. Mar. Pollut. Bull. 173, 113095.
He, D., Luo, Y., Lu, S., Liu, M., Song, Y., Lei, L., 2018. Microplastics in soils: Analytical methods, pollution characteristics and ecological risks. TrAC Trends Anal. Chem. 109, 163–172.
Herrera, M., Matuschek, G., Kettrup, A., 2003. Fast identification of polymer additives by pyrolysis-gas chromatography/mass spectrometry. J. Anal. Appl. Pyrolysis. 70 (1), 35–42.
Huang, Y., He, T., Yan, M., Yang, L., Gong, H., et al., 2021. Atmospheric transport and deposition of microplastics in a subtropical urban environment. J. Hazard. Mater. 416, 126168.
I. S. O. ISO. 2020. Environmental aspects-State of knowledge and methodologies. *ISOTR 21960*.
Käppler, A., Windrich, F., Löder, M.G.J., Malanin, M., Fischer, D., et al., 2015. Identification of microplastics by FTIR and Raman microscopy: a novel silicon filter substrate opens the important spectral range below 1300 cm−1 for FTIR transmission measurements. Anal. Bioanal. Chem. 407 (22), 6791–6801.
Kernchen, S., Löder, M.G.J., Fischer, F., Fischer, D., Moses, S.R., et al., 2022. Airborne microplastic concentrations and deposition across the Weser River catchment. Sci Total Env. 818.
Kershaw, P., Turra, A., Galgani, F., others. 2019. Guidelines for the monitoring and assessment of plastic litter and microplastics in the ocean.
Klein, M., Fischer, E.K., 2019. Microplastic abundance in atmospheric deposition within the Metropolitan area of Hamburg, Germany. Sci. Total Environ. 685, 96–103.
Knobloch, E., Ruffell, H., Aves, A., Pantos, O., Gaw, S., Revell, L.E., 2021a. Comparison of Deposition Sampling Methods to Collect Airborne Microplastics in Christchurch, New Zealand. Water. Air. Soil Pollut. 232 (4), 133.
Knobloch, E., Ruffell, H., Aves, A., Pantos, O., Gaw, S., Revell, L.E., 2021b. Comparison of Deposition Sampling Methods to Collect Airborne Microplastics in Christchurch, New Zealand. Water Air Soil Pollut. 232 (4).
Liao, Z., Ji, X., Ma, Y., Lv, B., Huang, W., et al., 2021. Airborne microplastics in indoor and outdoor environments of a coastal city in Eastern China. J. Hazard. Mater. 417, 126007.
Liu, Z., Bai, Y., Ma, T., Liu, X., Wei, H., et al., 2022c. Distribution and possible sources of atmospheric microplastic deposition in a valley basin city (Lanzhou, China). Ecotoxicol. Environ. Saf. 233, 113353.
Liu, X., Lu, J., He, S., Tong, Y., Liu, Z., et al., 2022b. Evaluation of microplastic pollution in Shihezi city, China, using pine needles as a biological passive sampler. Sci. Total Environ. 821, 153181.
Liu, S., Shang, E., Liu, J., Wang, Y., Bolan, N., et al., 2022a. What have we known so far for fluorescence staining and quantification of microplastics: A tutorial review. Front. Environ. Sci. Eng. 16 (1), 8.
Liu, K., Wang, X., Wei, N., Song, Z., Li, D., 2019. Accurate quantification and transport estimation of suspended atmospheric microplastics in megacities: Implications for human health. Environ. Int. 132, 105127.
Liu, K., Wang, X., Fang, T., Xu, P., Zhu, L., Li, D., 2019a. Source and potential risk assessment of suspended atmospheric microplastics in Shanghai. Sci. Total Environ. 675, 462–471.
Luo, H., Xiang, Y., Zhao, Y., Li, Y., Pan, X., 2020. Nanoscale infrared, thermal and mechanical properties of aged microplastics revealed by an atomic force microscopy coupled with infrared spectroscopy (AFM-IR) technique. Sci. Total Environ. 744, 140944.
Lux, L., Phal, Y., Hsieh, P.-H., Bhargava, R., 2022. On the Limit of Detection in Infrared Spectroscopic Imaging. Appl. Spectrosc. 76 (1), 105–117.
Mani, T., Hauk, A., Walter, U., Burkhardt-Holm, P., 2016. Microplastics profile along the Rhine River. Sci. Rep. 5 (1), 17988.
Mattsson, K., Jocic, S., Doverbratt, I., Hansson, L.-A., 2018. Nanoplastics in the Aquatic Environment. In: Microplastic Contamination in Aquatic Environments. Elsevier, pp. 379–399.
Nematollahi, M.J., Zarei, F., Keshavarzi, B., Zarei, M., Moore, F., et al., 2022. Microplastic occurrence in settled indoor dust in schools. Sci. Total Environ. 807, 150984.
O'Brien, S., Okoffo, E.D., O'Brien, J.W., Ribeiro, F., Wang, X., et al., 2020. Airborne emissions of microplastic fibres from domestic laundry dryers. Sci. Total Environ. 747, 141175.
Organization WH. 1997. Determination of airborne fibre number concentrations : a recommended method, by phase-contrast optical microscopy (membrane filter method).
Oßmann, B.E., 2021. Microplastics in drinking water? Present state of knowledge and open questions. Curr. Opin. Food Sci. 41, 44–51.
Page, M.J., McKenzie, J.E., Bossuyt, P.M., Boutron, I., Hoffmann, T.C., et al., 2021. The PRISMA 2020 statement: an updated guideline for reporting systematic reviews. BMJ. n71.
Peñalver, R., Costa-Gómez, I., Arroyo-Manzanares, N., Moreno, J.M., López-García, I., et al., 2021. Assessing the level of airborne polystyrene microplastics using thermogravimetry-mass spectrometry: Results for an agricultural area. Sci. Total Env. 787.
Plastics ISO. 2020. Environmental aspects-State of knowledge and methodologies. *ISOTR 21960*.
Prata, J.C., Reis, V., da Costa, J.P., Mouneyrac, C., Duarte, A.C., Rocha-Santos, T., 2021. Contamination issues as a challenge in quality control and quality assurance in microplastics analytics. J. Hazard. Mater. 403, 123660.
Qu, H., Diao, H., Han, J., Wang, B., Yu, G., 2023. Understanding and addressing the environmental risk of microplastics. Front. Environ. Sci. Eng. 17 (1), 12.
Rahman, L., Mallach, G., Kulka, R., Halappanavar, S., 2021. Microplastics and nanoplastics science: collecting and characterizing airborne microplastics in fine particulate matter. Nanotoxicology. 15 (9), 1253–1278.
Renner, G., Nellessen, A., Schwiers, A., Wenzel, M., Schmidt, T.C., Schram, J., 2019. Data preprocessing & evaluation used in the microplastics identification process: A critical review & practical guide. TrAC Trends Anal. Chem. 111, 229–238.
Rocha-Santos, T., Costa, M.F., Mouneyrac, C. (Eds.), 2022. Handbook of Microplastics in the Environment. Springer International Publishing, Cham.
Rousseau, R.M., 2001. Detection limit and estimate of uncertainty of analytical XRF results. Rigaku J. 18 (2), 33–47.
Scheurer, M., Bigalke, M., 2018. Microplastics in Swiss Floodplain Soils. Environ. Sci. Technol. 52 (6), 3591–4358.
Soltani, N.S., Taylor, M.P., Wilson, S.P., 2021a. Quantification and exposure assessment of microplastics in Australian indoor house dust. Environ. Pollut. Barking Essex 1987 (283), 117064.
Soltani, N.S., Taylor, M.P., Wilson, S.P., 2021b. Quantification and exposure assessment of microplastics in Australian indoor house dust. Environ. Pollut. 283, 117064.
Stanton, T., Johnson, M., Nathanail, P., MacNaughtan, W., Gomes, R.L., 2019. Freshwater and airborne textile fibre populations are dominated by 'natural', not microplastic, fibres. Sci. Total Environ. 666, 377–389.
Szewc, K., Graca, B., Dołęga, A., 2021a. Atmospheric deposition of microplastics in the coastal zone: Characteristics and relationship with meteorological factors. Sci. Total Environ. 761, 143272.
Szewc, K., Graca, B., Dołęga, A., 2021b. Atmospheric deposition of microplastics in the coastal zone: Characteristics and relationship with meteorological factors. Sci Total Env. 761.
Tondl, G., Bonell, L., Pfeifer, C., 2018. Thermogravimetric analysis and kinetic study of marine plastic litter. Mar. Pollut. Bull. 133, 472–547.

Trainic, M., Flores, J.M., Pinkas, I., Pedrotti, M.L., Lombard, F., et al., 2020. Airborne microplastic particles detected in the remote marine atmosphere. Commun. Earth Environ. 1 (1), 64.
Turner, A., Holmes, L., 2011. Occurrence, distribution and characteristics of beached plastic production pellets on the island of Malta (central Mediterranean). Mar. Pollut. Bull. 62 (2), 377–381.
Vandenabeele, P., 2013. Practical Raman Spectroscopy - An Introduction: Vandenabeele/Practical Raman Spectroscopy - An Introduction. John Wiley & Sons Ltd, Chichester, UK.
Vianello, A., Jensen, R.L., Liu, L., Vollertsen, J., 2019. Simulating human exposure to indoor airborne microplastics using a Breathing Thermal Manikin. Sci. Rep. 9 (1), 8670.
Wampler TP, ed. 2006. *Applied Pyrolysis Handbook*. CRC Press. 0 ed.
Wang, X., Li, C., Liu, K., Zhu, L., Song, Z., Li, D., 2020. Atmospheric microplastic over the South China Sea and East Indian Ocean: abundance, distribution and source. J. Hazard. Mater. 389, 121846.
Welsh, B., Aherne, J., Paterson, A.M., Yao, H., McConnell, C., 2022. Atmospheric deposition of anthropogenic particles and microplastics in south-central Ontario. Canada, Sci Total Env, p. 835.
Wieboldt D. 2010. Understanding Raman spectrometer parameters.
Wright, S.L., Levermore, J.M., Kelly, F.J., 2019. Raman Spectral Imaging for the Detection of Inhalable Microplastics in Ambient Particulate Matter Samples. Environ. Sci. Technol. 53 (15), 8947–8956.
Wright, S.L., Ulke, J., Font, A., Chan, K.L.A., Kelly, F.J., 2020. Atmospheric microplastic deposition in an urban environment and an evaluation of transport. Environ. Int. 136, 105411.
Xie, Y., Li, Y., Feng, Y., Cheng, W., Wang, Y., 2022. Inhalable microplastics prevails in air: Exploring the size detection limit. Environ. Int. 162, 107151.
Xu, G., Cheng, H., Jones, R., Feng, Y., Gong, K., et al., 2020. Surface-enhanced Raman spectroscopy facilitates the detection of microplastics< 1 μm in the environment. Environ. Sci. Technol. 54 (24), 15594–15603.
Yao, Y., Glamoclija, M., Murphy, A., Gao, Y., 2022. Characterization of microplastics in indoor and ambient air in northern New Jersey. Environ. Res. 207, 112142.
Zhang, Q., Zhao, Y., Du, F., Cai, H., Wang, G., Shi, H., 2020. Microplastic fallout in different indoor environments. Environ. Sci. Technol. 54, 11, 6530–6539.
Zhang, G.S., Liu, Y.F., 2018. The distribution of microplastics in soil aggregate fractions in southwestern China. Sci. Total Environ. 642, 12–20.

Glossary

Term: Definition
Active sampling: Collecting suspended particles through a device that requires the use of a pump to actively pass air through an air sample container
Airborne particle: Small particles that can be suspended in the atmosphere
Atmosphere: Covering layer of the earth stretches from the surface of the planet up to as far as 10,000 km (6,214 miles) above
Crosswind: Any wind that is perpendicular to the direction of travel.
Density altitude: The air density is given as a height above sea level.
Density separation: The technique to separate plastic particles based on the differences of density between plastics and non-synthetic materials
Fiber-shaped microplastics: Cylindrical microplastics with a length-to-width ratio of ≥3
Film-shaped microplastics: Irregular shape with 2 dimensions
Filter pretreatment: The procedure of cleaning filters before starting the experiment to reduce contamination.
Foam-shaped microplastics: Sponge-like texture
Fragment-shaped microplastics: Irregular shape with 3 dimensions having a length-to-width ratio of < 3
FTIR: Fourier transform infrared that is an infrared spectroscopy and analyutical technique
GC: Gas chromatography which is an analytical technique used to separate and detect the chemical components of a sample mixture that can vaporized without decomposition.
Heat stress index: It measures how a given air temperature feels to the average person at a given relative humidity (also known as comfort index)
Hit quality index: Index to show similarity between sample and reference spectrum
ISO: International Organization for Standardization
Limit of detection: The lowest possible unit (size/concentration) at which the method can detect within the matrix with a certain degree of confidence
MS: Mass spectroscopy, analytic technique by which chemical substances are identified by the sorting of gaseous ions in electric and magnetic fields according to their mass-to-charge ratios.
Matrix: The compartment where M/NPs are detected
Microplastic (MP): The plastic particle with a size range between 1 and 5 mm
Micro rubber: The finest polymeric particles from tire abrasion
Nano plastic (NP): The plastic particle smaller than 1 μm
Non-urban: Rural or environmental zone
Passive sampling: Collecting suspended particles through a device that relies on the kinetic energy of particulate matter to be settled on the surface
Planetary boundary layer (PBL): The lowest part of the atmosphere which is 3500 m above sea level (a.s.L.) or ~2800 m above ground level
Plastic: A synthetic material made from a wide range of organic polymers that can be molded into a shape while soft and then set into a rigid or slightly elastic form.
Psychro wet-bulb temperture: This is the temperature indicated by a moistened thermometer bulb exposed to the airflow.
Pyr-GC/MS: Pyrolysis–gas chromatography–mass spectrometry (Py-GC–MS) is a analytical technique where a sample is broken down into smaller stable components through controlled thermal degradation
Raman: An analytical technique which is based on the interaction of light with the chemical bonds within a material.
Relative humidity: A ratio of the amount of atmospheric moisture present relative to the amount that would be present if the air were saturated
Rubber: An elastic substance obtained from the exudations of certain tropical plants (natural rubber) or derived from petroleum and natural gas (synthetic rubber)
Station pressure: This is the pressure that is observed at a specific elevation and is the true barometric pressure of a location
TGA-MS: Thermogravimetric analysis- mass spectroscopy is a technique to study the thermal behavior of solid and liquid samples along with to characterizing and quantifying the compounds in the off-gas.
topography: The study of the forms and features of the surface
Urban area: Cities or towns with high-density population
Wind chill temperature: It is based on the rate at which exposed skin loses heat due to wind and cold